



Review

Plasmonic-based nanomaterials for environmental remediation

Dawei Wang^a, Suresh C. Pillai^c, Shih-Hsin Ho^d, Jingbin Zeng^e, Yi Li^{a,*}, Dionysios D. Dionysiou^{b,*}^a Key Laboratory of Integrated Regulation and Resource Development of Shallow Lakes, Ministry of Education, College of Environment, Hohai University 210098, PR China^b Environmental Engineering and Science Program, Department of Chemical and Environmental Engineering, University of Cincinnati, Cincinnati, OH 45221, USA^c Nanotechnology and Bio-Engineering Research Division, Department of Environmental Science, School of Science, Institute of Technology Sligo, Ash Lane, Sligo, Ireland^d State Key Laboratory of Urban Water Resource and Environment, School of Municipal and Environmental Engineering, Harbin Institute of Technology, Harbin 150090, PR China^e College of Science, China University of Petroleum (East China), Qingdao 266580, PR China

ARTICLE INFO

ABSTRACT

Keywords:

Photocatalysis

Toxicology

Silver

Gold

Pollutants

Emerging Contaminants

Technologies based on nanomaterials are gaining increased attention as a promising method for the removal of contaminants and inactivation/killing of pathogenic microorganisms. Plasmonic nanomaterials prove to be promising in this field due to their tailored properties, including optical, photothermal, conducive, and catalytic properties. These properties have been widely used for the design of efficient materials for the environmental applications by improving the light absorption efficiency, redox reaction kinetic rates, and charge separation efficiency. In the current review, the tailored properties of plasmonic nanomaterials and how they are employed for the design of efficient environment-functional materials are discussed in detail. A number of examples for the development of composite plasmonic nanostructures such as metal/semiconductor, metal/insulator/semiconductor, and metal/semiconductor/semiconductor are provided.

In addition, the recent achievements in plasmonic nanomaterials for the removal of contaminants (in both liquid and gaseous media) and the inactivation of pathogenic microorganisms are described with a number of examples. The major challenges in employing plasmonic nanomaterials for environmental applications are identified as: (1) complete mineralization of contaminants must be achieved in some cases due to the potential risks of intermediates; (2) the cost of plasmonic nanomaterials and the associated treatment processes need to be significantly decreased; (3) the stability of plasmonic nanomaterials in real environmental matrices is urgently needed to be improved; (4) the ecological safety of these nanomaterials should be investigated extensively. However, it is expected that with continuous progress of this field, plasmonic nanotechnology can be used for environmental applications more widely, not only for the examples shown in the current review, but also for soil remediation, resource recovery during waste treatment processes, and detection of contaminants. Finally, the toxicity of engineered plasmonic nanomaterials, the possibility of their release, fate, and transformation, in the environment and subsequent impact on the health of ecosystem are also addressed in detail.

1. Introduction

Environmental pollution due to the population growth and rapid industrialization of the developing regions has become a critical issue in recent times. The development of civilization has caused pollution of air, soil and water, which significantly poses threats to both human health and ecological safety. For example, water pollution causes approximately 14,000 deaths per day in developing countries, mostly because of drinking water contamination [1,2]. Some emerging contaminants which cannot be removed by traditional water treatment processes are now causing serious concerns [3,4]. Numerous scientific and technological efforts have been made to resolve these problems

[5,6]. Among all the approaches, technologies based on nanomaterials are playing an increasingly important role. Early efforts on developing nanomaterials for contaminant removal mainly focused on photocatalysis for the degradation of industrial dyes [7,8]. More recently, several emerging organic contaminants such as endocrine disrupting chemicals and pharmaceutical effluents and personal care products have also been chosen to be the target contaminants since they are not effectively treated by conventional water treatment processes [9,10]. So far, technologies based on nanomaterials have also been used to address environmental issues of aqueous contaminants [11,12], oil spills [13] and air pollutants [14]. Some practical applications have been developed, such as the fabrication of TiO₂-coated glass, which is

* Corresponding authors.

E-mail addresses: envly@hhu.edu.cn (Y. Li), dionysios.d.dionysiou@uc.edu (D.D. Dionysiou).

antifogging and self-cleaning [15]. In addition, the environmental applications of photocatalysis have expanded to a wider scope, including self-cleaning of buildings, inactivation and detection of microorganisms, and detection of pollutants [16]. It is also reasonable to believe that this scope will continue to expand since increasingly more severe environmental problems are emerging worldwide.

About two decades ago, “plasmonics”, was coined for a promising new technology that enables active manipulation of light by metallic nanomaterials [17]. Currently, plasmonics, an emerging interdisciplinary science and technology field, is being considered as a silver bullet for its potential applications in many sectors including environmental engineering [18]. The principles that drive plasmonics have been introduced most comprehensively in some recent review papers [18–20]. Since many classical review papers have summarized the achievement of plasmonic nanomaterials in terms of synthesis and applications, the current review discusses the progress of this field with a specific focus on what kind of environmental concerns plasmonic materials can help address.

Surface plasmon resonance (SPR) is related to the collective oscillations of conduction electrons in metals and it can be classified into two modes: propagating surface plasmons and localized surface plasmons [18]. Nanostructures that support surface plasmons experience a uniform electromagnetic field when excited by light as their dimensions are much smaller than the wavelength [21]. On the other hand, for nanostructures that possess at least one dimension close to the excitation wavelength, electromagnetic field is not uniform and surface plasmons propagate back and forth between the ends of the structures [22]. Thus, by tailoring the dimension, morphology and ambient environment of a metal, the latter can exhibit many fantastic optical properties [23,24], which offers new opportunities to the application of plasmonics in environmental sector [25]. The principle motivation for the current review is to explore the plasmonic applications in environmental remediation and their undergoing mechanisms (Fig. 1). We start from the properties of plasmonic nanomaterials (Section 2), such as optical, photothermal, conductive, and catalytic properties. Then we introduce how these properties are employed to design highly efficient nanomaterials for removal of contaminants (Section 3), and inactivation of bacteria (Section 4). Furthermore, the relevant physics and chemistry, recent achievements, and significant challenges in this field are be reviewed.

2. Plasmonic properties

2.1. Optical properties

One of the most attractive properties of plasmonic nanostructures is their strong light absorption efficiency, as reflected in their intense

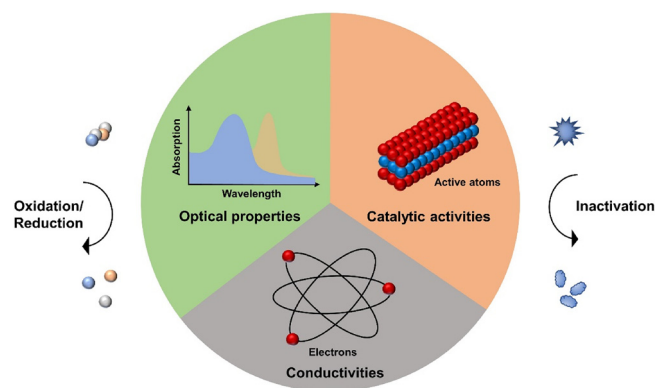


Fig. 1. Schematic illustration of the properties of plasmonic nanomaterials and their applications in the photocatalytic oxidation/reduction of pollutants and inactivation of bacteria.

color. When plasmonic nanoparticles are irradiated with light, the oscillating electromagnetic field induces a collective coherent oscillation of the free electrons (from conduction band) [18]. The specific wavelength where amplitude of oscillation reaches at maximum usually varies with metal types, shapes, and dimensions. Thanks to the marvelous achievements in the material science, morphologies of gold or silver nanoparticles can be controlled efficiently [26]. The varying morphologies, including spheres, rods, plates, and other geometries, as shown in Fig. 2, have helped the tuning of absorption wavelength across the visible range.

Generally, there are four methods to tune the optical properties of plasmonic nanostructures. Increase of size usually results in the red shift of absorption peak (Fig. 3a). For example, the increase in the diameters of gold nanoparticles could result in red-shift of SPR wavelength [43]. By tuning the aspect ratio of gold nanorods, a shift of absorption wavelength can be expected [44].

The second way is to fabricate composite structure, such as core/shell and Janus nanostructures, to manipulate the dielectric constants of the surrounding environment of plasmonic nanoparticles (Fig. 3b). For example, Wang et al. tuned the optical properties of Au@Cu₂O core/shell nanoparticles systematically by varying the thickness of Cu₂O shell [45]. They found that the plasmonic peaks red-shift continuously with the increase of Cu₂O shell thickness. This red-shift comes with the increase of shell thickness, which is further ascribed to the change of the refractive index of the surrounding medium. Similar effect was also observed for Au or Ag NPs coated with SiO₂ nanoshell, SiO₂ shell led to the red-shift of several tens of nanometers due to the increase refractive index of SiO₂ (1.43) in comparison to that of H₂O (1.33) [46]. In contrast, a blue-shift was observed by them when they progressively increased the voids between Au NPs and Cu₂O shell, which can be attributed to the decrease of the refractive index of the medium surrounding the Au NPs. Similar change of optical properties is also observed for Janus nanostructures [47].

The third way is to tune the morphology of plasmonic nanoparticles (Fig. 3c). For example, the absorption peak of isolated Au nanospheres usually lies around 520 nm, varying with its size. However, for isolated Au nanorods, besides the peak near 520 nm, a coupling peak at longer wavelength is also observed. Other morphologies as shown in Fig. 2. all demonstrate essentially different optical properties compared to spheres.

The forth way is to assemble isolated nanoparticles into secondary nanostructures (Fig. 3d). The differences between the optical properties of assembled nanostructures from that of their individual counterparts are caused by the different resonance modes. In assembled plasmonic nanostructures, individual plasmonic oscillations on nearby particles can couple via their near-field interaction and generate coupled plasmonic resonance modes [51]. Of particulate interest is the reversible assembly of such plasmonic nanostructures, which is expected to enable the dynamic tuning of the coupling peaks of SPR by external stimuli, and therefore benefit applications for detection [52]. In the case of the self-assembly of gold nanoparticles, one can observe a color change from red to blue, suggesting the formation of a linear chain structure. The formation of the chain structure is due to the balance between van der Waals attraction and electrostatic interaction among Au nanoparticles [27]. Meanwhile, gold nanorods are able to assemble in the forms of side-to-side and end-to-end, inducing variable optical changes [53].

In terms of plasmonic optical properties, silver offers more advantages over gold. Silver is able to support a strong surface plasmon across from 300 to 1200 nm, wider than gold is [18]. The well-controlled synthesis of silver nanostructures has achieved the full tuning of adsorption wavelength across visible-spectrum. By synthesizing silver with different morphologies including nanodisks and nanoprisms, Yin et al. observed a shift of absorption wavelength from 450 nm to 871 nm [54]. However, the susceptibility of elemental Ag to oxidation often leads to the unexpected changes of their morphologies and thus of their

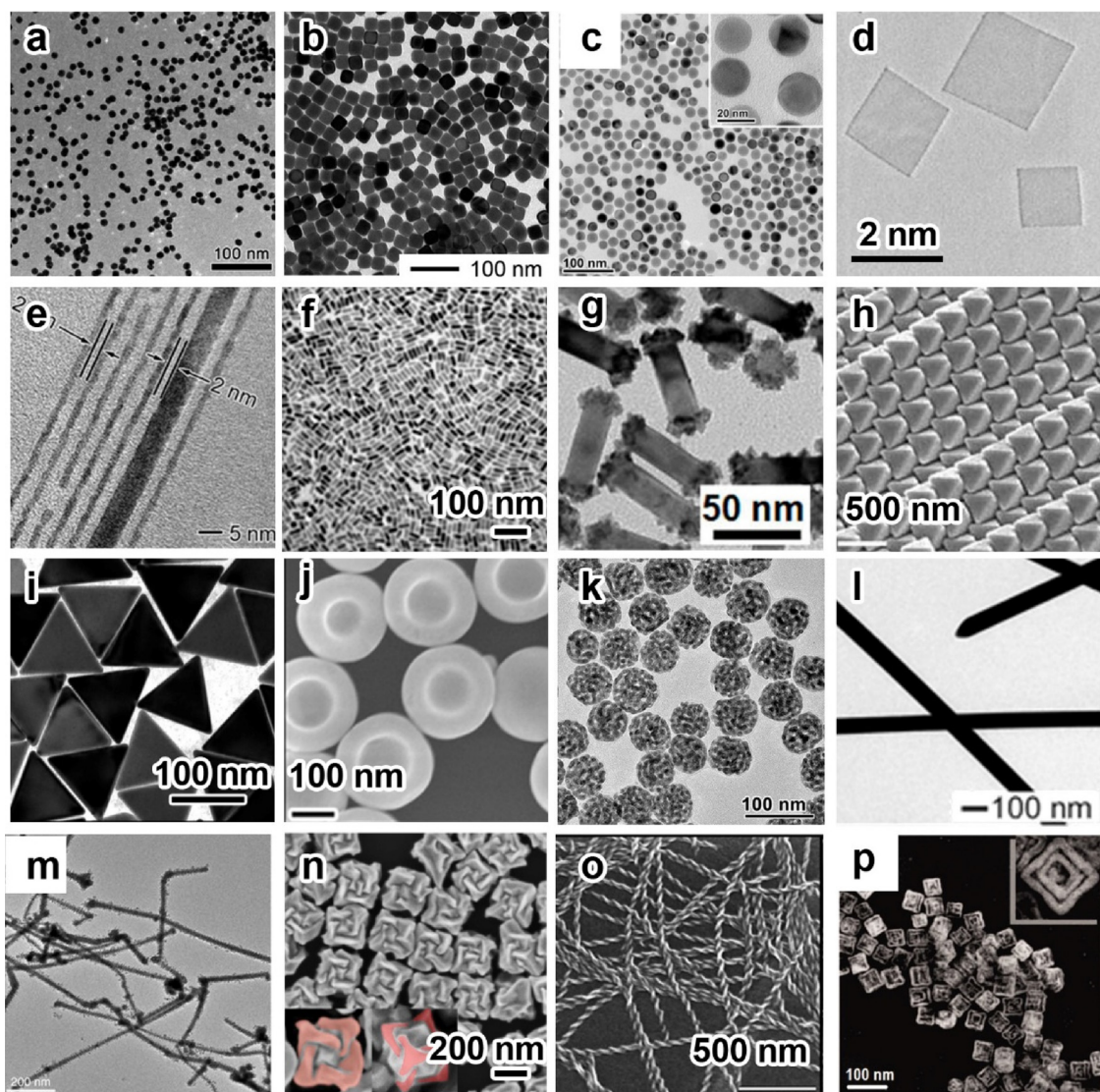


Fig. 2. TEM images of different gold/silver nanostructures. (a) Gold nanospheres, reprinted from Ref. [27], copyright 2011 American Chemical Society. (b) Silver nanocubes, reprinted from Ref. [28], copyright 2010 American Chemical Society. (c) Gold/silver alloy nanoparticles, reprinted from Ref. [29], copyright 2014 American Chemical Society. (d) Gold nanosheet, reprinted from Ref. [30], copyright 2011 Springer Nature. (e) Gold nanowires, reprinted from Ref. [31], copyright 2008 American Chemical Society. (f) Gold nanorods, reprinted from Ref. [32], copyright 2004 American Chemical Society. (g) Pt on the tips of Au nanorods, reprinted from ref. [33], copyright 2014 American Chemical Society. (h) Silver octahedrals, reprinted from Ref. [34], copyright 2012 Springer Nature. (i) Gold nanoprisms, reprinted from Ref. [35], copyright 2014 American Chemical Society. (j) Gold nanocup, reprinted from Ref. [36], copyright 2017 Wiley-VCH. (k) Porous gold/silver alloy shell, reprinted from Ref. [37], copyright 2016 American Chemical Society. (l) Silver nanowires, reprinted from Ref. [38], copyright 2004 American Chemical Society. (m) Epitaxial gold nanowires, reprinted from Ref. [39], (n) chiral gold nanoparticles, reprinted from Ref. [40], copyright 2011 Springer Nature. (o) Double-helical gold nanowires, reprinted from Ref. [41], copyright 2018 American Chemical Society. (p) Double-walled gold/silver nanoboxes, reprinted from Ref. [42], copyright 2018 The American Association for the Advancement of Science.

optical properties, hindering the potential applications. In materials science, this drawback could be overcome by depositing a layer of gold due to its resistance to oxidation. By carefully controlling of the deposition process to avoid the galvanic reaction between Ag and HAuCl_4 , Qin et al. achieved depositing an ultrathin layer of Au on the Ag nanocubes [55]. After depositing the thin layer of Au, the extinction of the Ag nanocubes only changed slightly, meanwhile, the Au layer could prohibit Ag nanocubes from the oxidation of H_2O_2 . Besides direct deposition, one can also improve the stability of Ag nanostructures while maintaining their optical properties by alloy process. Yin et al. synthesized fully alloyed Ag/Au nanospheres through a surface protected annealing process. They firstly deposited a layer of silver on gold nanospheres, then they coated the core/shell nanoparticles with SiO_2 to protect them from sintering during annealing process. Through this process, they obtained alloyed nanospheres with significantly narrow

bandwidths, and notable stability in harsh environments [29].

In short, because of the above mentioned optical properties, plasmonic nanostructures have received significant attention for the design of visible-light driven photocatalysts. The controllable resonant wavelength region of plasmonic nanostructures has been expected to benefit the improvement of incident light absorption, which can help the development of environment-functional nanomaterials.

2.2. Photothermal properties

Photothermal properties are associated with optical properties. The response to near-infrared (NIR) light of plasmonic nanostructures has been proven to be promising to generate thermal power. One of the earliest demonstrations of the photothermal properties of plasmonic nanostructures is the morphological transformation of gold nanorods

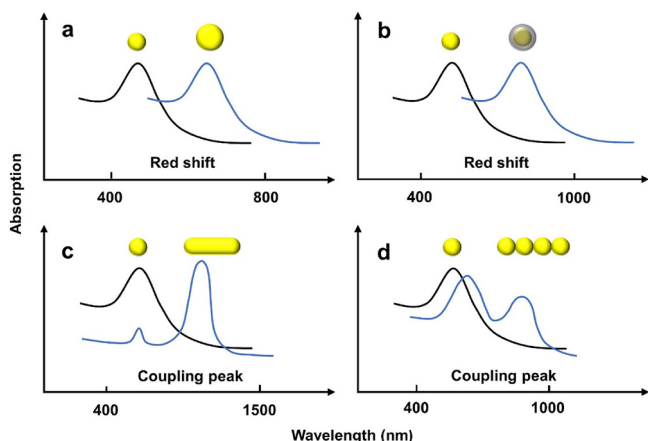


Fig. 3. Different methods for tuning the optical properties of plasmonic nanostructures: (a) size control: the increase of size usually results into the red shift of plasmonic peak. For example, the peak of Au nanoparticles can be tuned from ~ 500 to 700 nm by increasing the size from 17 nm to 150 nm [48]. The size control of Au nanorods can even extend the peak to infrared region. (b) Introduction of composite structure, including core/shell and Janus structures: this method is highly independent on the refractive index of the counterpart. (c) Morphology change: the longitudinal peak (at longer wavelength) of gold nanorods can be easily tuned to 1400 nm [49]. (d) Assembly into secondary nanostructure: the assembly of gold nanoparticles can result to a coupling peak at ~ 700 nm [27], while the end-to-end assembly of gold nanorods can make the coupling peak go to as far as 1000 nm [50].

under pulsed laser irradiation. In this study, El-Sayed et al. found that gold nanorods could turn into nanospheres with femtosecond laser irradiation. They also observed a melting process, which suggests the high temperature of the particles when they are under the laser irradiation [56]. This phenomenon, which has been recognized as photothermal effect, is due to SPR. It is known that SPR excitations dramatically increase the yield of conduction electrons that are raised from a ground state to an excited state [20]. These electrons interact with the electrons of the metal lattice elevating the lattice temperature. When this interaction comes down to nanoscale, the light-to-heat conversion can be highly efficient [57]. Recently, this mechanism has been applied to the synthesis of highly uniform Au nanorods [58].

Since the plasmonic excitation is relevant to the morphology and size of the nanostructures, the photothermal properties can also be tuned by controlling these two parameters. Theoretical calculations have verified the morphology dependent photothermal properties of gold nanostructures [59]. Simultaneously, it has also been demonstrated that the increase of temperature of gold nanoparticles is proportional to their sizes [60]. However, for isolated plasmonic nanoparticles, the photothermal effect is not that significant compared to their corresponding assembled structures. For example, Qiu et al. calculated the temperature field distribution around a gold nanoparticle with 50 nm radius in water. Under the irradiation of 530 nm light (intensity = 1 mW/ μm^2), the temperature of the gold nanoparticle increases to 52 °C. On the contrary, when a few gold nanoparticles are assembled into an array, the temperature can increase up to 800 °C [61].

One of the most exciting benefits of the photothermal effect is the possibility to boost overall reaction kinetics. Since most chemical reactions can be accelerated by increasing temperature according to Arrhenius equation ($k = Ae^{-E_a/(RT)}$, where k is the rate constant, T is the absolute temperature, A is the pre-exponential factor, E_a is the activation energy, and R is the universal gas constant) [57]. Moreover, it has been proposed that the local heating resulting from photothermal effect gives a better catalytic effect than the bulk heating [62]. In the environmental sector, the photothermal effect has been utilized to improve the degradation rate of contaminants [63] and the inactivation of

bacteria and viruses [64]. Recently, photothermal effect of plasmonic nanoparticles has been used to vaporize water into steam [65], which is a clean water source.

2.3. Other properties

In addition, plasmonic metals are also excellent electrical conductors. For example, the electrical conductivity of bulk gold is 4.10×10^7 S/m, while for bulk silver its conductivity is as high as 6.30×10^8 S/m, which is even higher than that of bulk copper (5.96×10^7 S/m) [66]. This excellent electrical conductivity of plasmonic metals does not decrease much when their sizes are in the nanoscale regime, making them promising for various electrical-related applications. The satisfactory conductivity of plasmonic nanostructures has been taken into advantage for the design of efficient photocatalysts by facilitating the charge separation [67].

Moreover, some plasmonic metals are also of satisfactory catalytic properties, and are being used in various industrial applications. One of the demonstrations is the catalytic converter. Due to the incomplete combustion of fuel, the exhaust usually includes a toxic mixture of CO, NO_x , SO_x , and hydrocarbons (C_xH_x). The plasmonic metal, platinum, has been used to convert these flue gases into non-toxic gases such as CO_2 , N_2 , and H_2O [68]. However, the reactions with conventional catalysts are usually operated at elevated temperatures or pressures. Recently, the fantastic optical properties of plasmonic materials have allowed them to use light energy to drive catalytic reactions, which is a promising approach to address the issues of energy efficiency and stability of catalysts [69].

3. Visible-light driven photocatalysts

The remarkable achievements associated with the plasmonic materials have enabled wide applications, such as the design and synthesis of efficient photocatalysts. Photocatalysts with plasmonic subunits have been used in water splitting [70], photovoltaics [71], and environmental remediation [72], etc. In this section, we mainly discuss the development of the design of photocatalysts for environmental remediation. We start from the introduction on the design principles, and then summarize the achievement of plasmonic photocatalysts in remediation of water and air issues.

To tackle various issues of environmental pollution, semiconductors are among the most promising photocatalysts [73]. However, most semiconductors (e.g. TiO_2 and ZnO) can only be activated under UV light regardless of the magnificent achievement on their synthesis (Fig. 4a). When photon energy of greater than or equal to the bandgap energy of semiconductor is illuminated onto its surface, the h^+/e^- pairs are photoexcited in femtoseconds [74]. These holes and electrons will produce a series of reactive oxygen species (ROS) to decompose the organic pollutants (Fig. 4b) [75]. Numerous attempts have been devoted in the past three decades to improve the performance of semiconductor photocatalysts, particularly for the higher absorption of

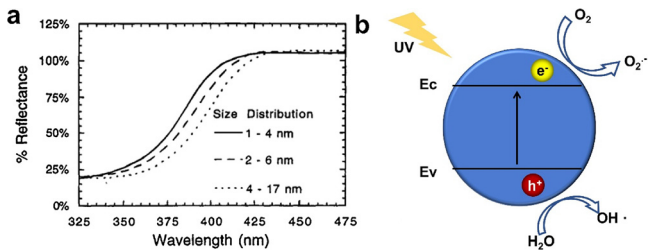


Fig. 4. (a) UV/vis reflectance spectra of size-quantized TiO_2 . Reprinted with permission from Ref [73]. Copyright 1995 American Chemical Society. (b) Photo-induced formation electron-hole pairs in a semiconductor particle.

visible light by doping other materials. Among those attempts, decorating plasmonic metals on semiconductors has attracted significant attention. It can be expected that through proper control, the full-spectrum photocatalysis can be achieved since the SPR wavelength of Ag and Au is highly tunable [76].

The tunable properties of plasmonic nanostructures have guided the design of efficient plasmonic photocatalysts. Plasmonic photocatalysts with different composites have been proposed and proven to be promising. In terms of plasmonic photocatalysts, there are typically three types of design principles: metal/semiconductor, metal/insulator/semiconductor, and metal/semiconductor/semiconductor. Different compositions may correspond to different activation mechanisms. It should be noted that some of these mechanisms were firstly proposed in other fields, rather than environmental engineering. In consequence, our discussion in this section may also expand to water splitting and solar cells, where plasmonic nanomaterials are also widely used.

3.1. Effect of composition and geometry arrangement

3.1.1. Metal/semiconductor direct contact

In 1997, Sayama and Arakawa introduced Pt as a co-catalyst on TiO_2 and observed a significant enhancement of photocatalytic efficiency [77]. Since then, numerous studies have investigated the effect of plasmonic metals including Au [78–80] and Ag [81–85] on photocatalysis enabled by semiconductor under light irradiation. In those early days, methanol was used as sacrificial agents to trap the photo-generated holes to further allow the electrons to initiate some reduction reactions, while the role of noble metal was only considered to accelerate the hole-electron separation (Fig. 5a) [78]. Kamat et al. found that photoexcitation of TiO_2 under UV illumination resulted in accumulation of the electrons in Ag as evidenced from the shift in the surface plasmonic resonance band [86,87]. This mechanism was further verified using nanosecond laser flash photolysis [86]. By exciting the Au@ TiO_2 using 308 nm laser pulse, they observed the absorption band at 420 nm and photobleaching at 540 nm as the result of the electron storage on Au [86]. However, this theory cannot explain the excellent performances of metal/semiconductor under visible light irradiation since most conventional semiconductors can only be excited under UV irradiation. Soon after that, Tian and Tatsuma found that the curves for conversion efficiency from incident photon to electron in solar cells with Au- TiO_2 as photoanode matched the absorbance spectrum of the incorporated Au nanoparticles [88]. However, it was an exactly different phenomenon from previous studies which considered metal NPs as a sink for charge carriers [89]. The authors carried out spectroscopic measurements and found that the absorbance changes at 680 nm for Au- TiO_2 increased gradually under the visible light irradiation [88]. This phenomenon was similar with that for TiO_2 when it is applied with a more negative potential [90]. So they proposed that the charge separation was achieved by electron transfer from the excited Au NPs to TiO_2 [88]. This mechanism was also verified by measuring the incident photon to current conversion efficiency (IPCE) of an Au/ TiO_2 Schottky diodes, in which a continuous flow of electrons from gold to TiO_2 was observed [91]. These works are valuable for understanding the SPR effect on the metal/semiconductor system, but they still did not present

the direct evidence of SPR induced electron transport from plasmonic nanoparticles to TiO_2 . In contrast, Furube et al. used femtosecond IR probing to observe electrons injected from the plasmon band of Au nanodots that were attached to TiO_2 NPs [92]. They found that the electron transport time was within 240 fs, and the yield was about 40%. This ultrafast plasmonic induced electron transfer was also observed in Ag/AgCl system, in which AgCl acted as a semiconductor [92]. Recently, DuChene et al. discovered that these plasmonic induced electrons possessed excited-state lifetimes much longer than those of electrons which are photogenerated directly on TiO_2 under UV irradiation [93]; they attributed this phenomenon to the significant Schottky barrier [91,94,95] established at the Au/ TiO_2 interface (Fig. 5b). They explained that although this Schottky barrier mitigates the transportation of hot electrons (e.g. the high-energy electrons produced by photoirradiation [96], “hot” here refers to “energetic” [97]) into the TiO_2 conduction band, once the barrier was breached, the depletion layer within the semiconductor facilitated charge separation by discarding these electrons from the interface between Au and TiO_2 [93]. However, Priebe et al. suggested this mechanism was resulted from the collaboration of different electron excitation pathways with Au particle, namely d-sp inter-band transitions in the lower and SPR transitions in the longer wavelength [98]. Similar phenomenon was also observed by Gomes Silva et al., but they attributed that to the nanometric size of the noble metal particle and the operation of quantum size ambiguously [99]. In fact, metal size indeed plays a significant role in determining the bending the semiconductor bands according to a recent study [100]. Recently it has also been proven that at most 95% of the effective charge carriers came from the decay from surface plasmon to hot electrons [101].

During this period, some studies attempting to accelerate this SPR induced electron transport from a noble metal to a semiconductor were also carried out. Kang et al. incorporated photonic crystal to tune light-matter interactions and observed that more hot electrons were produced within Au NPs and injected into the conduction band of TiO_2 [102]. The composites of plasmonic metals and some other semiconductors such as Cu_2O [103], Fe_2O_3 [104] and CeO_2 [105] etc. have also been reported for record performance. However, despite these achievements, the charge recombination, which was highly dependent on the particle size of TiO_2 , was also observed: larger TiO_2 NPs were accompanied by longer charge recombination period due to the longer diffusion length of electrons in those TiO_2 NPs. Recently, Lin et al. found that the photocatalytic activity also depends on the facet of the semiconductor in the neighborhood of plasmonic metals [106].

An interesting question that could be raised is that how the electrons transfer when the metal/semiconductor system is irradiated by UV and visible light simultaneously. By measuring the photocurrent of Ag/ TiO_2 film under solar light irradiation, Takai and Kamat found that direct excitation of Ag nanoparticles played negligible effect under such condition [87]. In contrast, because the zero-current potential of Ag/ TiO_2 shifted to more negative potential compared to pristine TiO_2 , the benefit of plasmonic nanoparticles in this case was mainly contributed to Fermi level equilibration due to the electron storage in Ag nanoparticles. However, this theory is not universal because Fermi level equilibration can be greatly affect by the arrangement, type, and size of plasmonic metals and semiconductors [107–110].

3.1.2. Metal/insulator/semiconductor contact

Despite the significant achievements in photocatalysis by introducing plasmonic nanostructures, some problems are not addressed: many energetic charge carriers recombine rather than participating in photocatalytic reactions [70]. Although the intense electric fields formed around the plasmonic metal nanostructures could increase the formation rate of e^-/h^+ pairs at the nearby semiconductor [111], the recombination and back electron transfer cannot be suppressed efficiently. Moreover, “bare” metal nanostructures especially Ag may corrode [112]. So an ideal core-shell configuration is highly desired

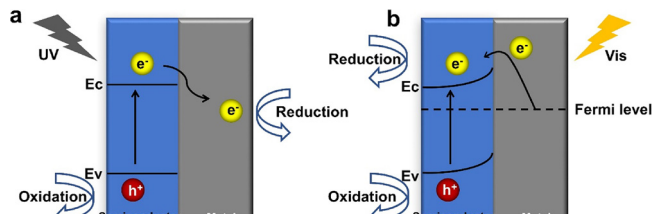


Fig. 5. Two different mechanisms of photocatalysis over noble metal/semiconductor particles (a) under UV and (b) visible light irradiation.

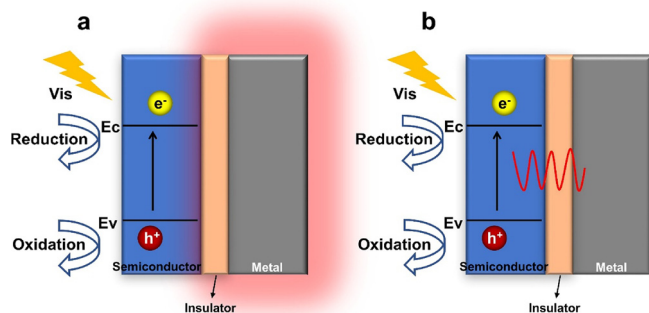


Fig. 6. (a) enhancement of local electrochemical field and (b) resonant energy transfer introduce the generation of charge carriers in the semiconductors nearby plasmonic nanoparticles.

[113]. Standidge et al. proposed an insulator shell to overcome the corrosion of bare metal [112]. Similar strategies were also proposed by Domen group in 2006 [114–117]. Awazu et al. coated SiO_2 shell on Ag NPs and embedded them in TiO_2 layers to prevent the oxidization of Ag [118]. Nevertheless, it was unclear of the charge transfer between plasmonic nanoparticles and the semiconductors in the presence of insulator. One of the mechanisms is that the enhancement of local electromagnetic field surface due to plasmonic resonance contributed to the local generation of electron-hole pairs in the semiconductor (Fig. 6a) [70,112,119]. However, because the local electromagnetic field can only create carriers for energies higher than the band gap of the semiconductor, only limited materials are appropriate. Another mechanism is resonant energy transfer (RET, Fig. 6b). RET produces e^-/h^+ pairs in the semiconductor by dipole-dipole interactions between plasmonic nanoparticles and semiconductors. Wu et al. investigated this mechanism by testing the photocatalytic performance of $\text{Au}@\text{SiO}_2@\text{Cu}_2\text{O}$ sandwich nanoparticles and using transient-absorption spectroscopy, in which 100-fs pulses excite the plasmon and detect the carriers created in the conduction band of Cu_2O [120]. This mechanism initiated some attempts of aligning plasmonic metals with some emerging semiconductors which were unconventionally used to take advantage of the plasmonic effect [121–124].

3.1.3. Metal/semiconductor/semiconductor (heterojunction) contact

Another efficient strategy to improve the separation between electrons and holes is to introduce heterojunction. Generally, heterojunction is defined as the interface between two different semiconductors with unequal band structure [125]. The re-alignments of band gaps at the interface can facilitate the charge separation. Specifically, when two semiconductors, A and B, are in contact, if the conduction band and the valance band levels of A are higher than that of B, the photogenerated electrons in A are able to transfer to B, while the photogenerated holes travel in an opposed direction, enabling an efficient charge separation. So far, various heterojunction schemes have been proposed, such as type-II, p-n, surface, and direct Z-scheme [126,127]. With the help of plasmonics, the photocatalysis performance of the heterojunction system can be further improved by either introduction of visible light driven activity, or more efficient generation of electrons due to plasmonic effect [128–130]. For example, Li et al. presented a sandwiched $\text{CdS}-\text{Au}-\text{TiO}_2$ nanorod array as the photoanode for water splitting and they proposed a dual working mechanism which extends the photoconversion wavelength from 525 to 725 nm: (1) Au NPs acted as an electron sink, which facilitated the charge transfer between CdS and TiO_2 under the irradiation of short wavelength light; (2) Au NPs initiated RET process when they were irradiated by long wavelength light [131].

Besides above-mentioned three strategies, some other plasmonic composites have also raised attention, including metal/metal/semiconductor [33] and plasmonic nanoarrays/semiconductor [132,133]. However, as we noted, some of the pieces of evidence on the charge

transfer involved in the plasmonic photocatalysis are indirect, suggesting that further mechanistic investigation is urgently needed [134].

3.2. Effect of morphology

It has been noted that for the design of plasmonic photocatalysts, not only the composition and geometry arrangement, but also the morphology of the components is highly important. As we have discussed in Section 2, the morphology of plasmonic nanomaterials can affect their optical properties, and thus the photocatalytic activity when light is used to activate the photocatalysts. For example, Ye et al. achieved broadband visible and even near-infrared light harvesting over gold nanorods/ TiO_2 by tuning the aspect ratio of gold nanorods [76]. Recently, Ma et al. assembled $\text{Au}@\text{Ag}$ nanoparticles into nanochain structure to improve the light absorption efficiency and thus the photocatalytic activity [135]. A recent study also investigated the morphological effect using gold nanospheres, nanorods, and nanostars on the photocatalytic performance of $\text{SiO}_2/\text{Au}/\text{TiO}_2$ system, and found that the nanostars demonstrated the highest activity due to the field enhancement at the spikes [136]. Meanwhile, the morphology control over the plasmonic nanomaterials can also significantly change the number of active sites for catalysis [137,138] and the efficiency of charge separation process [139].

It should be noted that the composition of semiconductors in the plasmonic photocatalysts can also alter the charge transfer since different semiconductors have different bandgaps. However, even for the same semiconductor, the morphology control can significantly improve the performance of plasmonic photocatalysts. For example, Ozin and co-workers reported inverse opals composed of anatase nanocrystals of TiO_2 can serve as efficient photocatalysts when the stopband energy is optimized with respect to the anatase absorption [140]. When the photonic bandgap of the inverse opals is tuned to overlap the absorption region of plasmonic nanoparticles, a more significant improvement on photocatalytic activity can be achieved [141–143]. Similar strategy was adopted by Wang et al. to use chiral TiO_2 nanowires to increase the light absorption of silver nanoparticles [144].

4. Removal of contaminants

4.1. Removal of contaminants from water matrix

With plasmonic photocatalysts, dyes, persistent organic pollutants [145], and endocrine disrupting chemicals [144] can be removed effectively under visible light irradiation [72,146]. Excellent photocatalysts should decompose pollutants rapidly but also remain stable themselves. However, plasmonic metals usually suffer from their poor stability during catalytic reactions, which has limited their practical applications [147]. Core-shell (metal-semiconductor) structures may overcome this disadvantage. Yin et al. synthesized an effective and stable catalyst that assembled a SiO_2 core, a layer of gold NPs, and a doped nanocrystalline TiO_2 shell [148]. A higher photocatalytic activity was observed than the catalyst without gold NPs, which implies the charge separation ability of Au. However, this advantage may be eliminated if excessive amounts of Au are mixed as this may increase the recombination rate [70,149]. Not only the amount of plasmonic nanoparticles, but also their size affects the photocatalytic performance [150]. Wu et al. demonstrated that $\text{Ag}@\text{Cu}_2\text{O}$ core-shell heterostructure is an efficient visible-light photocatalyst, due to its light absorption over the entire visible light region, which can be achieved by adjusting the shell thickness [151]. They attributed this enhancement to both direct electron transfer and resonant energy transfer. Recently, Au and Ag alloy also exhibited this potential as Au owns a relatively strong stability and Ag has more tunable SPR wavelength [152].

Moreover, some emerging photocatalysts have also exhibited high stability. Among them, Ag deposited on AgCl (referred as Ag/AgCl below) has been proven to be highly stable and active under the

irradiation of visible light [153]. The mechanism of this system is that under the irradiation of visible-light, electron-hole pairs are generated in Ag. Because of the strong electronic coupling between Ag and conduction bands of AgCl, photo-generated electrons in Ag injects into AgCl rapidly and efficiently, producing ROS [92]. Meanwhile, since AgCl is terminated by Cl^- ions and thus negatively charged, the holes transferred to the surface of AgCl, oxidizing Cl^- to Cl^0 atoms [153]. Both $\cdot\text{OH}$ and Cl^0 oxidize pollutants and reduce Cl^0 back to Cl^- , rapidly reproducing Ag, and thus stabilizing the Ag/AgCl system [144]. Similarly, Ag/AgI and Ag/AgBr have also been found to be stable and active under irradiation of visible light [154,155].

4.1.1. Organic contaminants

Dyes are widely used in many industries such as textile and papermaking. However, the presence of vat dyes, acetic acid, sulphur, naphthol, soaps, nitrates, enzymes, chromium compounds and heavy metals such as arsenic, cadmium, copper, lead, nickel, mercury, and cobalt and certain auxiliary chemicals make the dye effluent highly toxic [156]. As a result, the dye degradation experiment has been selected as the widely accepted demonstration for the photocatalytic activity. Meanwhile, the color changes also make it easy to monitor the dye degradation process. Below is a short list of studies on the plasmonic photocatalysts for dye degradation (Table 1). Various dyes, including Acid orange 7, Methyl orange, Methylene blue, and Rhodamine B, are used as target contaminants for the demonstration of the photocatalytic performance. However, a critical point to note is that the complex photochemistry of dyes could make the mechanistic discussion on the photocatalysis misleading. This is due to the fact that some dyes can induce photosensitization in the catalysts involved [157]. Valid conclusion can only be drawn when a control experiment is performed under identical conditions [134].

In terms of plasmonic photocatalysts, different plasmonic metals, including silver and gold, have been studied. The types of co-catalysts, which are usually semiconductors, have been expanded. Not only TiO_2 , which is the most widely used semiconductor, silver halides, C_3N_4 , copper oxides with various structures including nanotubes, nanowires, and hollow spheres, have been investigated (Fig. 7).

Moreover, the development of material science has also opened more choices for the design of plasmonic photocatalysts. For example, by introducing iron oxides, magnetic properties can be introduced and make the photocatalysts recyclable [163]. As an excellent electricity conductor and adsorbent, carbon nanotubes [164], graphene and its related composites (graphene oxide and reduced graphene oxide) [165,166] have also been incorporated. The improvement of photocatalytic performance accompanied by graphene is ascribed to its superior electron mobility and high specific surface area, which make it a perfect station for photogenerated electrons [167]. Meanwhile, metal organic frameworks (MOFs) as emerging materials with superior surface area, have also been incorporated in the design of efficient

plasmonic photocatalysts [168]. The large surface area can help capture more organic molecules to enhance the subsequent oxidation rate [169]. It is expected that with the continuous progress in material science, more choices will be available toward the development of efficient tailor-designed visible light-active photocatalysts.

A detailed map of the dye degradation mechanism is also critically important. For the photocatalytic oxidation of organic compounds, the typical mechanism is that the photogenerated ROS oxidize organics into CO_2 and H_2O [73]. The type of ROS also affects the product selectivity. The identification of ROS is thus important to map out the reaction mechanism, which can be achieved by dosing different quenching agents and comparing their corresponding impacts. For example, methanol, NaHCO_3 , and *p*-benzoquinone can be used to quench $\cdot\text{OH}$, h^+ , and $\cdot\text{O}_2^-$, respectively [178]. On the other hand, other techniques such electron paramagnetic resonance [179] and fluorescence detection [180] can be adopted as well to probe the radical species.

Besides dyes, some contaminants of emerging concern (CEC) have also been given considerable attention. Among them, endocrine disrupting chemicals (EDCs) and pharmaceuticals and personal care products (PPCPs) are of high concerns [181]. These CEC are widely detected in the effluents of wastewater treatment plants and even in natural waters [3,9]. More importantly, some of these CEC may not be effectively eliminated in conventional wastewater treatment processes [182]. To address these issues of CEC, plasmonic photocatalysts have also been applied (Table 2).

However, some studies have found that the photocatalytic oxidation reactions can only decompose organic compounds with large molecular weight (MW) into organic compounds with small MW, and only parts of the latter could be eventually mineralized into CO_2 and H_2O [184]. Some of these intermediates still have toxicity [192,193]. As a result, the evaluation of photocatalytic degradation of the CEC usually involves several other analyses besides the determination of contaminant concentration. For example, total organic carbon has been used to assess the mineralization rate, and estrogenic activity has been employed to evaluate the remaining toxicity of the photocatalytic effluent of EDCs contained water [194].

4.1.2. Inorganic contaminants

The photogenerated holes with oxidizing capacities have been used to decompose organic contaminants, while the photogenerated electrons have shown promising potential in some reductive reactions. Two representative examples would be heavy metals and nitrate [195–199]. The release of heavy metals such as copper, cadmium, and lead from industrial processes is frequent, thus threatening the ecosystem [195]. Nitrate can cause serious human health problems and eutrophication in natural waters [198].

Review of the redox potentials may help us understand how the plasmonic photocatalysis achieves the removal of heavy metals. Table 3 shows the redox potentials of several ubiquitous metal ions. To initiate the reduction of heavy metals, the metal ions should own a less negative reduction potential than the conduction band of the photocatalysts (e.g. conduction band of TiO_2 is -0.2 V , which may vary slightly with pH) [201]. Consequently, in theory, Cu^{2+} , Ag^+ and $\text{Cr}_2\text{O}_7^{2-}$ can be readily reduced by photocatalysis method, while the other three ions cannot be reduced. In fact, most studies on the photocatalytic remediation of heavy metal contamination, including those related to plasmonic photocatalysis, choose Cr(VI) as target heavy metal ion. For example, Su et al. fabricated magnetic triple-shelled nanoparticles ($\text{Ag}@\text{Fe}_3\text{O}_4@\text{SiO}_2@\text{TiO}_2$) and used them for photocatalytic reduction of $\text{Cr}_2\text{O}_4^{2-}$ [202]. They observed an improved reduction efficiency of their triple-shell nanoparticles compared to P25, TiO_2 nanospheres, and $\text{Fe}_3\text{O}_4@\text{SiO}_2@\text{TiO}_2$, which was attributed to the increased light absorption from Ag.

However, the photocatalytic reduction of Cr(VI) to Cr(III) is generally inefficient since the photogenerated holes cannot be timely consumed [203]. Wang et al. conducted a systematic study on the effect

Table 1
Short list of studies on dye degradation with plasmonic photocatalysts.

Dye	Photocatalyst	References
Acid orange 7	$\text{AgCl}@\text{Ag}@\text{TiO}_2$	[170]
Basic fuchsin	$\text{Ag}/\text{AgVO}_3@\text{g-C}_3\text{N}_4$ nanosheet	[171]
Methylene blue	$\text{Ag}@\text{C}_3\text{N}_4$	[172]
Methylene blue	$\text{Ag}_3\text{PO}_4/\text{AgBr}/\text{Ag-HKUST-1}$	[168]
Methylene orange	$\text{Ag}@\text{AgCl}$ cubic cage	[92]
Methylene orange	$\text{Ag}@\text{AgCl}@\text{TiO}_2$ nanotubes	[173]
Methylene orange	Au/TiO_2	[80]
Methylene orange	$\text{Ag}/\text{AgX}/\text{GO}$ ($\text{X} = \text{Br, Cl}$)	[174]
Methylene orange	$\text{Ag}@\text{Cu}_2\text{O}$	[175]
Rhodamine B	$\text{Au}/\text{Reduced Graphene Oxide}/\text{TiO}_2$	[167]
Rhodamine B	$\text{Au}/\text{N-TiO}_2$	[148]
Rhodamine B	Ag-TiO_2 hollow spheres	[176]
Sulforhodamine B	$\text{Au}/\text{Zeolite-Y}$	[177]

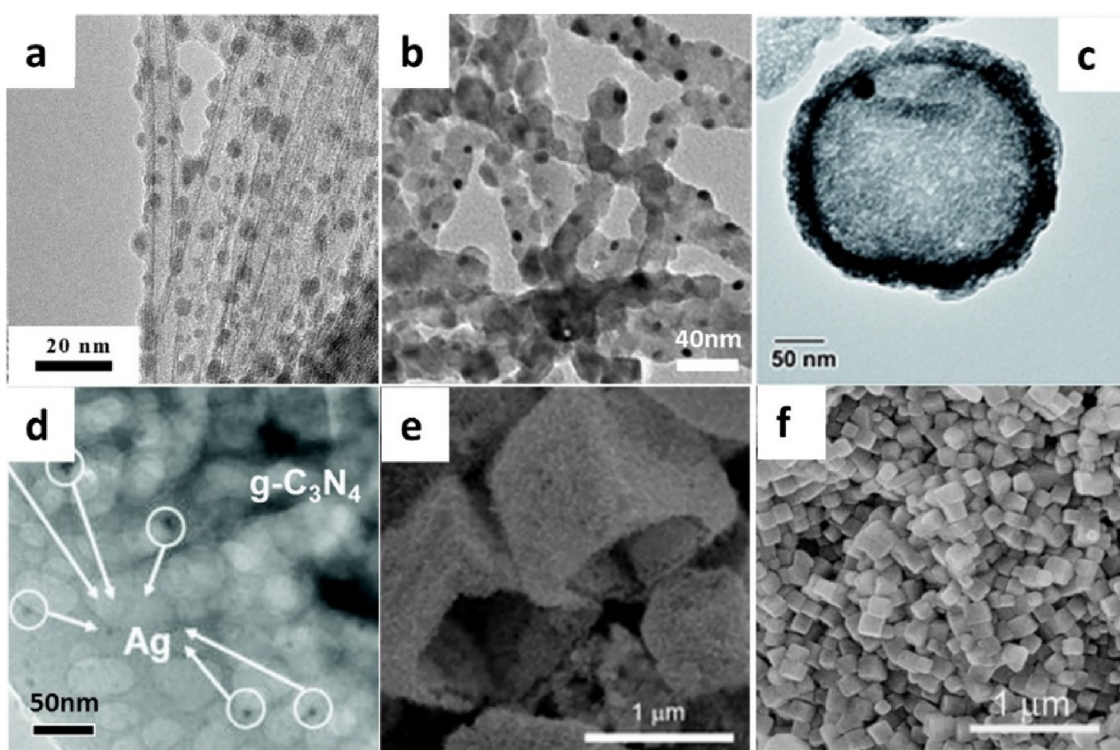


Fig. 7. Various plasmonic metals/semiconductor composites: (a) Ag@TiO₂ nanotubes. Reprinted with permission from [158]. Copyright 2015 American Chemical Society. (b) Ag/AgCl@TiO₂ nanofibers. Reprinted with permission from [144]. Copyright 2013 Royal Society of Chemistry. (c) Au@TiO₂ yolk-shell nanostructure. Reprinted with permission from [159]. Copyright 2013 Royal Society of Chemistry. (d) Ag/g-C₃N₄ composite. Reprinted with permission from [160]. Copyright 2016 Royal Society of Chemistry. (e) Au-CuO nanocages. Reprinted with permission from [161]. Copyright 2011 Royal Society of Chemistry. (f) Ag/AgCl nanocubes. Reprinted with permission from [162]. Copyright 2012 Wiley-VCH.

Table 2

Short list of studies on the removal of ECs with plasmonic photocatalysts.

ECs	Photocatalyst	Reference
17 α -ethinylestradiol	Ag/AgCl@Chiral TiO ₂ nanofibers	[144]
17 α -ethinylestradiol	Ag/ZnO	[183]
17 β -estradiol	Pt/P-TiO ₂	[184]
17 β -estradiol	Pt/Pd on cells	[185]
2,4-dichlorophenol	Ag/TiO ₂	[186]
2,4-dinitrophenol	Ag/CuO/TiO ₂	[187]
Bisphenol A	Ag/Reduced graphene oxide	[188]
Bisphenol A	Ag/AgBr@Fe ₂ O ₃	[189]
Bisphenol A (BPA)	Au/Bi ₄ Ti ₃ O ₁₂	[190]
chlorophenol	Ag-AgI/Al ₂ O ₃	[155]
Perchlorate	Pt/ruthenium-sensitized TiO ₂	[79]
Phenol	Pt/TiO ₂	[191]

Table 3

Redox potentials of metal ions (calculated based on Nernst Equation at pH = 3.0). Reprinted with permission from ref [200].

Electrode reaction	E°/V
Cd ²⁺ + 2e ⁻ → Cd	-0.40
Ni ²⁺ + 2e ⁻ → Ni	-0.24
Pb ²⁺ + 2e ⁻ → Pd	-0.13
Cu ²⁺ + 2e ⁻ → Cu	0.34
Ag ⁺ + e ⁻ → Ag	0.80
Cr ₂ O ₇ ²⁻ + 14H ⁺ + 6e ⁻ → 2Cr ³⁺ + 7H ₂ O	0.88

of small molecular weight organic acids on the photocatalytic reduction of Cr(VI), and found that these organics which act as sacrificial agents can significantly improve the performance of the photocatalysis [204]. Commonly, researchers usually dose methanol or NaHCO₃ to consume

holes [195]. In addition, formic acid is also found to be significantly efficient as a dosing agent for the photocatalytic reduction of Cr(VI). For example, Wang et al. synthesized core/shell AuPd@Pd nanocrystals for the reduction of Cr(VI) in the presence of formic acid. They proposed that formic acid can be decomposed into H₂ by Pd, and H₂ can reduce Cr(VI) into Cr(III) [205].

Nevertheless, the cost of dosing sacrificial agents in real applications is high. On the contrary, several studies demonstrated that organic contaminants can also act as sacrificial agents to consume the photo-generated holes. For example, Zeng et al. used Au nanoparticles decorated TiO₂ nanotubes to reduce Cr(VI). Instead of formic acid or methanol, they used acid orange 7 (a type of dye) to react with the generated holes, resulting in the simultaneous removal of heavy metals and organic contaminants [206]. The Au nanoparticles in their study served as the sink of electrons, which facilitated the charge separation. Choi et al. also developed a similar system with Ag/TiO₂ to achieve the removal of 4-chlorophenol and Cr(VI) [207]. Notably, they intentionally separated the photocatalytic reduction and oxidation. Under light irradiation, the holes generated by Ag/TiO₂ firstly oxidize 4-chlorophenol, while the electrons are stored in the Ag nanoparticles. In the subsequent dark experiment, Cr(VI) is reduced by these stored electrons [207]. This phenomenon is remarkable since usually the life time of photogenerated electrons is short (less than milliseconds) [86,208]. This study may inspire the development of continuous removal of pollutants using both day and night (dark) cycles [207]. The reduction capacity of TiO₂ has also inspired some strategies for the synthesis of plasmonic nanostructures. The photocatalytic reduction of Ag⁺ and Au³⁺ has been used to deposit their corresponding nanoparticles on semiconductors, which shows improved photocatalytic performance compared to isolated semiconductors [209,210].

Not only heavy metals, but also plasmonic photocatalysts have been used for the removal of nitrate. In a recent review by Westerhoff et al.,

one can find the summary of photocatalysts used for the reduction of nitrate, including plasmonic photocatalysts [211]. The decoration of plasmonic nanoparticles on semiconductor not only improves the performance in terms of enhanced charge transfer and light absorption efficiency, but also changes the bandgap of the catalyst, which thus achieve the tuning of reduction products, such as ammonia or nitrogen [211].

4.1.3. Beyond

As shown above, plasmonic photocatalysis has been widely used in the remediation of environment, including applications for both organic and inorganic contaminants. It is noteworthy that the satisfactory performance of plasmonic photocatalysis has also enabled simultaneous removal of contaminants and resource recovery. For example, Lianos et al. synthesized Pt/CdS/TiO₂ to achieve H₂ production during the removal of organic contaminants. In their system, Pt acts as electron sink which facilitates the separation of holes and electrons. As a result, the reduction of H⁺ to H₂ takes place near the surface of Pt, while the holes on TiO₂ surface oxidize the organic contaminants [212]. A similar strategy has also been applied in some photoelectrochemical cells, where the oxidation and reduction reactions are separated. In a typical photoelectrochemical cell, a photocathode and a photoanode are connected to external circuit. Under light irradiation, electron/hole pairs are generated on the photoanode. The produced holes initiate oxidation reactions, whereas the electrons transfer to the photocathode to initiate reduction reactions. This concept has been widely used in studies for energy production, such as water splitting [213]. In the environmental sector, photoelectrochemical processes have been applied for the decomposition of organic contaminants, reduction of heavy metals, reduction of nitrate, disinfection, and energy production during wastewater treatment processes [214–216]. We note that even though plasmonic nanomaterials are widely explored for water splitting, they have rarely been used in the environmental remediation. Several examples are shown as follows: Wang et al. developed a photoelectrochemical cell with Ag/AgCl@chiral TiO₂ nanofibers as photoanode. The electrons transferred to the counter electron not only produce electricity, but also achieve production of hydrogen [196]. They also developed a cell to recycle heavy metal from wastewater by the photogenerated electrons [195]. Because of the tunable properties of plasmonic nanomaterials, the oxidizing and reducing capacities of cell that employed them as photoanode could be explored further for many redox reactions in environmental remediation. Moreover, we can expect with further progress in material science, more efficient resource recovery from wastewater can be achieved by plasmonic photocatalysts.

4.2. Remediation of air pollution

The development of plasmonic nanomaterials has also offered great opportunities for the removal of air pollutants. In this section, we introduce some recent progress in the removal of both organic and inorganic air pollutants over plasmonic nanomaterials. It should be noted that besides those air pollutants discussed in this section, some studies also investigated the potential of plasmonic related nanomaterials for the disinfection of bioaerosols. The disinfection of bioaerosols is discussed in Section 5, along with the discussion of waterborne bacteria and viruses.

The removal of air pollutants also relies on the redox reactions initiated by the photogenerated charges. The holes or the resulted ROS can oxidize some air pollutants, while the electrons can reduce some other pollutants. Since the underlying mechanisms are very similar to those for the remediation of water pollutants, in this Section, we mainly focus on the discussion on what kinds of air pollutants can be removed by plasmonic related materials.

4.2.1. Organic contaminants

Among numerous indoor air pollutants, such as particulate matter (PM), carbon monoxide, and biological pollutants, volatile organic compounds (VOCs) has been gaining increasing attention [217]. VOCs are ubiquitous in many indoor environments. More importantly, their concentrations are consistently higher indoors than outdoors [218]. Exposure to VOCs may cause serious symptoms [219,220]. The common methods to remove the VOCs include source control, increasing ventilation rates, and air cleaning [221]. Photocatalysis is currently being considered as an efficient way to control VOCs, while with plasmonic nanomaterials, the visible light driven photocatalytic degradation of VOCs has been achieved.

VOCs are defined as organic compounds with a boiling point ranging from 50 to 260 °C at atmospheric pressure and room temperature [222]. Formaldehyde (HCHO), toluene, acetaldehyde, and para-dichlorobenzene are some of the VOCs. They may come from flooring materials, painting and wood materials [223]. HCHO has small molecular weight and is believed to be decomposed relatively easily. Meanwhile, HCHO is considered as one of the most concerning VOCs. Thus, many studies chose it as target VOC for the demonstration of the photocatalytic performance of their materials. Fujishima et al. firstly used TiO₂ film for the photocatalytic degradation of gaseous HCHO [224]. Since then, many studies have reported the potential of different semiconductors for the photocatalytic degradation of HCHO. In 2005, He et al. reported the photocatalytic degradation of HCHO over Pt/TiO₂, where they found that Pt can significantly improve the performance, and more importantly, HCHO was totally mineralized into CO₂ and H₂O [225]. Later, different plasmonic nanoparticles, including Au and Ag, and various semiconductors, such as Al₂O₃, Fe₂O₃ and MnO₂ have been incorporated to the efficient photocatalytic degradation of HCHO [226]. Notably, not only the types of plasmonic metals and semiconductors, but also the crystal facet of semiconductor has a significant effect on HCHO oxidation. In photocatalytic studies dealing with CeO₂ loaded with Pd, Zhou et al. found that the [110] facet of CeO₂ can more efficiently oxidize HCHO into CO₂ than the [111] facet [227]. More recently, Wang et al. developed a composite of Au@ZnO@ZIF-8 for the simultaneous detection of removal of HCHO. In their system, ZIF-8 with high surface area can concentrate trace level of HCHO on the surface of ZnO. Under visible light irradiation, the electromagnetic field around ZnO was enhanced by Au nanorods, and facilitated the oxidation of HCHO [119].

Different from HCHO, other VOCs are more difficult to be decomposed. For example, the highly stable aromatic ring of toluene usually remains intact. The carbonyl group makes the phenyl ring even more inert since the conjugation effect decreases its electron density [223]. Consequently, the studies on the photocatalytic degradation of these VOCs usually involve investigations on the final products and how the incorporation of plasmonic materials affects product selectivity. For example, in studies on the photocatalytic oxidation of benzene over Pt/TiO₂, Einaga et al. demonstrated that the final oxidation products were composed by both CO₂ and CO. By modifying the ratio between Pt and TiO₂, the produced CO was further oxidized into CO₂ [228]. Even though they did not elucidate the detailed mechanism, their study indicates that the incorporation of plasmonic nanomaterials affects product selectivity. Similarly, Xu et al. reported that by introducing Ag/AgBr onto P25, most of benzene can be photocatalytic decomposed into CO₂. For pristine P25, the complete mineralization of benzene, however, was difficult to observe [229]. They found that for Ag/AgBr/P25, more ·OH can be formed. With the incorporation of Ag nanoparticles, the bandgap decreased to 2.9 eV from 3.5 eV of that for pristine P25. Meanwhile, Ag nanoparticles can greatly improve the charge relaxation time to 27 µs from 18 µs. Consequently, Ag/P25 photocatalyst can oxidize more benzaldehyde into CO₂ [230]. The incorporation of plasmonic materials also helps to maintain the activity of semiconductors. For example, Li et al. used Ag loaded α-Fe₂O₃ for the photocatalytic oxidation of benzene. The produced intermediates were

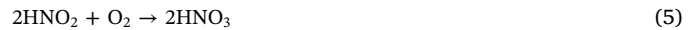
identified by *in-situ* Fourier transform infrared spectroscopy. They found that for pristine α -Fe₂O₃, benzene was firstly oxidized into benzaldehyde and benzoic acid, which may retain on the surface of catalyst and cause its progressive inactivation. However, with the doping of Ag nanoparticles, no intermediates were observed. Consequently, the Ag loaded α -Fe₂O₃ exhibited higher stability [231].

As shown above, numerous studies have demonstrated that the incorporation of plasmonic materials with semiconductors have greatly improved the photocatalytic degradation of VOCs, either by improving the stability of photocatalysts, or by facilitating the complete mineralization. However, the loaded amount of plasmonic nanomaterials should be optimized for this improvement. Kubacka et al. studied the photocatalytic degradation efficiency of toluene by tuning the loading amount of Ag on g-C₃N₄ and they found that with 1 wt% loading amount, the efficiency was the highest [232]. This was because excessive amount of Ag may act as recombination center for holes and electrons.

4.2.2. Inorganic contaminants

Major inorganic contaminants in air include carbon monoxide (CO), nitrogen containing compounds (NO_x), sulfur containing compounds (SO_x), and mercury (Hg). CO is colorless, odorless, and toxic gas. The oxidation of CO into CO₂ has been believed to be the most reliable way for its abatement in air. Even though CO is flammable, its concentration in contaminated air is very low, which means its complete combustion is impossible [233]. To achieve its remediation, it is thus necessary to accumulate CO and catalyze its subsequent oxidation. CO is a molecule with three resonance structures, which renders its exceptional adsorption to the surface of metal oxides and metals [233]. CaO, Al₂O₃, and Pt have been used for this purpose [234]. Gulari et al. used Pt/Al₂O₃ for the selective catalytic oxidation of CO. They also investigated the effect of H₂O and CO₂ on the catalytic oxidation, and found that the presence of H₂O can improve the reaction efficiency while CO₂ can poison the catalyst [235]. It should be noted that this study was carried out at elevated temperatures. To initiate the CO oxidation at room temperature, photocatalysis was later introduced. For example, Einage et al. reported the photocatalytic oxidation of CO over Pt/TiO₂. By investigating the reaction details, they found that Pt in this system serves as active sites for the chemical adsorption of CO [236]. More recently, it was found that the adsorbed CO reacts with Pt to form platinum carbonate. Interestingly, this reaction is reversible and thus make this reaction a catalysis process [237]. Not only Pt, but also other plasmonic metals, such as Au, have been used for this application. The incorporation of Au on TiO₂, Co₃O₄, ZnO, and Fe₂O₃ has been demonstrated for the catalytic oxidation of CO [238,239]. It is known that under light irradiation, plasmonic resonance helps produce thermal energy, which may help facilitate chemical reactions. Cronin et al. demonstrated that for Au/Fe₂O₃, the improved CO catalytic oxidation did not result from the thermal (plasmonic) heating alone [240]. On the other hand, the size of Au nanoparticles also has a significant effect on the photocatalytic oxidation of CO [241].

NO_x are also poisonous gases emitted primarily from fuel combustion. Their presence is of major environmental concern since they cause acid rain, photochemical smog, and ecological toxicity [242]. Since NO_x have complex chemical properties, both photocatalytic oxidation and reduction can be used for their remediation. In some cases, NO_x can be oxidized into nitrate ions in water. However, NO_x can also be reduced to N₂. Several reactions related to the oxidation of NO are presented below:



As shown above, the oxidation of NO can give some harmful intermediates. Consequently, for the photocatalytic oxidation of NO_x, a major interest is the control of the intermediates [243]. Huang et al. reported that with the modification of Ag nanoparticles, the perovskite oxide (SrTiO₃) showed an improved photocatalytic oxidation of NO into nitrate ions. Due to the plasmonic effect, abundant ROS were produced, which inhibited the generation of harmful intermediates [244]. Wang et al. reported that by calcination, Schottky contact between Ag and TiO₂ and oxygen vacancies on TiO₂ can be formed, which promoted the selective photocatalytic reduction of NO to N₂ [245]. SO_x are also harmful gases resulting from combustion of fuels. The removal of SO_x through photocatalysis is an emerging field [63,246,247], even though the studies on the plasmonic application in this field are very few [248].

Elemental mercury (Hg) species, as the predominant species in flue gas when burning lignite coals, are not efficiently controlled by available air pollution control devices [249]. Due to the high mobility and low solubility of Hg in water, the technologies for its abatement mainly focus on its oxidation. Composite plasmonic photocatalysts have been proposed for this application [248]. We note that Ag and its halides are the major plasmonic materials used for the photocatalytic removal of mercury [228,250]. The wide use of these materials is only partially attributed to the excellent optical and electrical properties of Ag and satisfactory catalytic activity of silver halides. More importantly, the amalgamation mechanism also helps the improved adsorption toward Hg [228]. It should be noted that many of the air pollutants come from the combustion of fuels. As a result, it is necessary to investigate their removal efficiency in the presence of multiple components. For instance, the effect of moisture and oxygen should be carefully considered [251].

5. Inactivation of microorganisms

Antimicrobial resistance is a continually growing problem as the usage of antimicrobial drugs increase, and bacteria have developed new mechanisms to combat these drugs that were designed to combat them [252]. It is therefore of utmost importance to develop novel methods and processes for disinfection against antimicrobial resistant organisms. Although disinfection methods currently used can efficiently control microbial pathogens, research in the past few decades has uncovered a dilemma between harmful disinfection byproducts and effective disinfection [253]. The significant achievement in nanomaterial science has shown a promising feature to re-invent the century-old conventional disinfection methods. Along with the potential of plasmonic nanoparticles previously mentioned in this review, many noble metal plasmonic nanoparticles, such as Ag or Au, often exhibit the additional benefit of antimicrobial properties. It is necessary to first look at the cell structures before we discuss the mechanism of photocatalytic disinfection. As shown in Fig. 8a, bacteria cell have very complex structures [254]. The compositions and roles of different cell components can be summarized as follows: (1) Some species of bacteria have a capsule, which is composed of carbohydrates. The role of capsule is to maintain hydration; (2) Cell wall is composed of protein-sugar molecules. The wall gives the cell its shape and surrounds the cytoplasmic membrane, protecting it from environment; (3) The cytoplasm of bacteria cells is where the functions for cell growth, metabolism and replication are carried out; (4) cytoplasmic membrane consist of a layer of phospholipids and proteins, which encloses the interior of bacteria and regulates the flow of materials in and out of the cell; (5) Flagella beat in a propeller-like motion to help the bacteria move toward nutrient and away from toxic chemicals; (6) Nucleoid is a region of cytoplasm where DNA is located; (7) Phil help bacteria attach to other cells and surfaces; (8) Ribosomes translate the genetic code from nucleic acid to amino acid [254]. Different bacterial cells may have various cellular wall

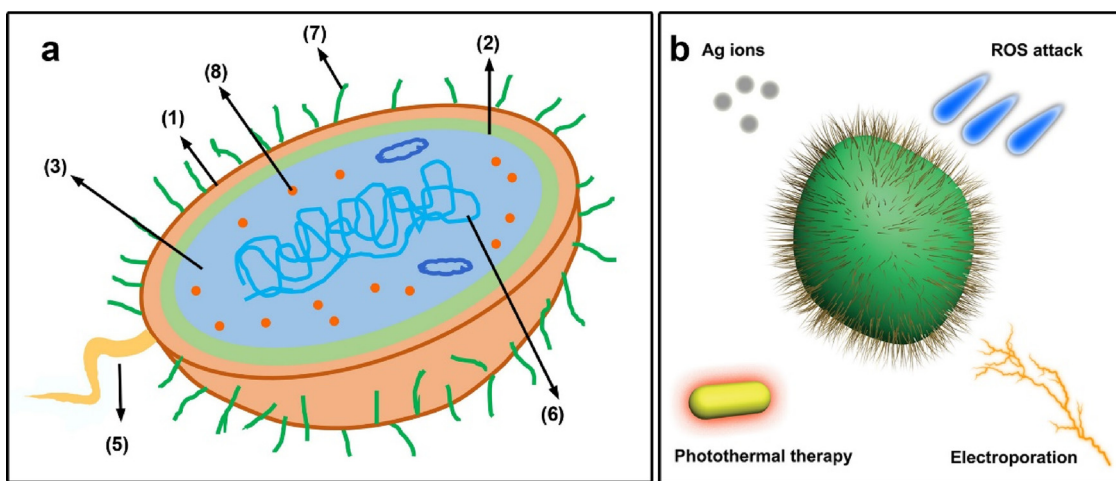


Fig. 8. (a) Typical structure of a bacterial cell. (b) Four typical mechanisms involved in the plasmonic nanomaterials-enabled inactivation of bacteria.

composition, and they are classified as Gram-positive and Gram-negative bacteria [255]. Previous studies have suggested that the plasmonic-based inactivation to bacteria may result in the damage of every single component of bacterial cells [255–257]. Rather than discussing the damage of the plasmonic nanomaterials cause to the components of cells, the discussion on the disinfection mechanism falls into four general categories: Ag, photocatalytic inactivation, photothermal inactivation, and electroporation (Fig. 8).

5.1. Silver

The antimicrobial capacities of silver have been recognized for a long time and used in many areas such as sterilization of medical devices [253]. Feng et al. presented a systematic study on the anti-bacterial effect of Ag^+ on *Escherichia coli* (*E. coli*) and proposed that the protein became inactivated and DNA lost its replication ability after the treatment of Ag^+ [258]. One of the earlier demonstrations of silver nanoparticles in environmental application is the inactivation of *E. coli* with the $\text{Ag-TiO}_2/\text{UV}$ system [259]. Sökmen et al. studied the photocatalytic disinfection of *E. coli* with Ag loaded TiO_2 . They found that the loading of Ag dramatically reduced the UV illumination time for the complete disinfection [259]. Even though they did not elucidate the detailed disinfection mechanism, their study has facilitated the investigation of this field. Soon after this study, Salopek-Sondi and Sondi investigated the disinfection capacity of Ag nanoparticles. *E. coli* was also used as target microorganism, but they did not use UV light [260]. They found that in the presence of Ag nanoparticles, the cells of bacteria were seriously damaged and “pits” were observed in the cell walls. They also investigated the element composition of the treated bacteria and observed the existence of Ag. Further TEM images confirmed that Ag nanoparticles were accumulated in the membrane, and many of them penetrated into the cells successfully [260].

Moreover, Ag ions could be produced because of the dissolution of Ag nanoparticles. Ag ions react with thiol groups in proteins, inactivating respiratory enzymes and also enabling the production of ROS [261]. Ag ions have also been reported to destroy the structure and permeability of cell membrane and prevent DNA replication [258]. However, it should be noted that Jeong et al. found the possible connection between disinfection performance and the bacteria species [262]. They found that Ag nanoparticles only showed mild inhibitory effect on *Staphylococcus aureus* (ATCC 19636), which is a Gram-positive bacterium, while Ag nanoparticle could effectively kill *E. coli* (Gram negative). They attributed this difference to the different peptidoglycan layer thicknesses of the membrane structures of Gram negative and Gram positive bacteria [262]. In addition, Guzman et al. found out that the size of Ag nanoparticles also influences the disinfection

performance, and smaller size shows better performance [263]. This is readily acceptable since for smaller Ag nanoparticles, more Ag atoms are exposed, which facilitates its release as Ag^+ . Based on this theory, it is of no surprise that not only Ag nanoparticles but also the nanocomposites of Ag, such as silver halides nanoparticles, exhibit antibacterial performance [264].

5.2. Photocatalytic disinfection

Photocatalysis has also been used for the disinfection of microorganisms. The fundamental mechanisms of this process rely on the ROS production driven by the light irradiation [265,266]. As already mentioned in Section 3, photocatalytic process can oxidize most of the organics. Notably, almost every part of cell is composed of organics, or contains organics at least. In fact, as much as 96% of the cell's dry weight is composed of organic macromolecules [265]. Within this context, photocatalytic disinfection may be attributed to the decomposition of cell structure by ROS. Cell membrane rupture caused by ROS has also been considered as the primary mechanism of photocatalytic disinfection process [267].

When ROS are produced around bacteria, the first barrier between them is the capsule. Extracellular polymeric substances are located near the cell surface, maintaining the hydration and providing a protective fence against environmental stress [268]. It was once hypothesized that the extracellular polymeric substances may prevent ROS from attacking the cell. Liu et al. demonstrated the protective function of extracellular polymeric substances by comparing the disinfection efficiencies of heterotrophic bacteria to the same bacteria without extracellular polymeric substances. Removing the extracellular polymeric substances by centrifugation increased the inactivation efficiency [269]. On the contrary, Sharon et al. found no observable effect of extracellular polymeric substances on the susceptibility of cells [270]. A more recent study suggested a dual function of capsular extracellular polymeric substances in the photocatalytic inactivation of *E. coli*, even though extracellular polymeric substances prevent cells from being attacked by ROS, these substances also facilitate photocatalytic inactivation by accelerating the adhesion of photocatalysts to the cell surface [271].

Photocatalysis may also disorder the cell wall of bacteria. Kiwi and Nadtchenko evaluated the effect of photocatalysis on phosphatidyl-ethanolcholine, peptidoglycan, and lipo-polysaccharide (LPS) of the *E. coli* membrane wall with FTIR [272]. Their results suggest that photocatalysis results in the disorder of LPS lipid layer and the peroxidation of LPS on TiO_2 is also faster than *E. coli*, suggesting that the LPS bilayer structure order determines the rate of photocatalytic peroxidation process. By comparing the peroxidation of three major components of the wall, they also found that PGN is the most resistant toward

peroxidation. With laser photolysis, they also found that the reaction between LPS, *E. coli* or phosphatidyl-ethanolcholine and holes competes with the recombination between holes and electrons [272].

The damage to cytoplasmic membrane is another major mechanism of the photocatalytic inactivation of bacteria. A few studies have shown the lipid oxidation and the release of cell content, such as potassium ions, RNA, and proteins, during the photocatalytic process [273,274]. By monitoring the death of *Saccharomyces cerevisiae* with flow cytometry and a double straining strategy, Guillard et al. suggested that cytoplasmic membrane constituted a key target of the ROS, which irreversibly damaged even in the presence of a thick cell wall [275]. DNA damage has also been considered as one of the primary mechanisms for photocatalytic inactivation. Dukan and Gogniat revealed that photocatalysis causes damage that becomes deleterious during recovering from photocatalytic stress, especially for mutants sensitive to ROS species [276].

Generally, the above studies have revealed that photocatalysis may destruct almost every single component of the cell. In fact, the photocatalytic inactivation of bacteria could be a step-by-step process. For example, ROS may first destruct the cell membrane, which increases the permeability of the cell membrane. Therefore, ROS could accelerate intracellular protein carboxylation and DNA degradation to ultimately cause bacterial death [277].

5.3. Plasmonic photothermal therapy

Even some plasmonic nanomaterials with excellent biocompatibility (e.g. Au) demonstrate their potential for selective inactivation, which is difficult for Ag and ROS. The response of plasmonic nanoparticles to NIR creates a localized heating effect that can be utilized in many disinfection applications, now termed as photothermal therapy [278]. The selective killing of cancer cells with gold nanoparticles is among the earliest demonstrations of the great potential of photothermal therapy [279]. The treatment of bacteria and viruses further shows the promise of this technology [280,281]. So far, the mechanism of photothermal inactivation of bacteria has been widely accepted: when the frequency of incident light overlaps with the plasmonic resonance of Au nanoparticles, the excited electrons result in non-equilibrium and rapid heating. The produced heat can kill cells through different ways, such as induction of heat-shock proteins, endothelial swelling, denaturation of proteins/enzymes, metabolic signaling disruption, and microthrombosis [64].

One of the advantages of Au nanoparticles-enabled photothermal disinfection is the selectivity. Various functional groups can be capped on the surface of Au nanoparticles, improving colloidal stability of Au nanoparticles in environmental media, e.g. aqueous and oil phase [36,282]. The anchor of these functional groups is attributed to the strong affinity between the gold atoms and these groups. For example, amino group, thiol group, carboxyl group, and phosphorus group all have strong affinity to Au atoms. On the other hand, some of these groups are essential components of biomolecules. Therefore, with appropriate surface modification, proteins, enzymes, DNA, and RNA can also be capped on the surface of Au nanoparticles [283–285].

The various surface functionalities of Au nanoparticles make them promising candidate for the conjugation with biomolecules. With the aid of different functional biomolecules, Au nanoparticles can selectively attach on the surface of target bacteria, and thus achieve the selective killing. For instance, Sabo-Attwood et al. used primary antibodies modified Au nanorods to selectively destroy the pathogenic Gram-negative bacterium, *Pseudomonas aeruginosa* (PA) [281]. By applying step-by-step surface modification, IgG-conjugated Au nanorods were produced. Without any antibody modification, very few of Au nanorods can land on the surface of bacteria. On the other hand, with antibody conjugation, the binding efficiency was significantly increased. When the solution of Au nanorods and bacteria was irradiated by NIR light (785 nm) for 10 min, the cell viability decrease by 75%

[281]. Similarly, Ray et al. reported popcorn shaped Au nanoparticles which are antibody-conjugated for the selective killing of drug-resistant *Salmonella typhimurium* DT104 bacteria. The antibody modified popcorn shaped gold nanoparticle can conjugate with bacteria efficiently. Thus, when they were irradiated by 670 nm laser, the photothermal effect led to a nearly 100% inactivation of bacteria [286].

Recently, the advantages of some unique nanostructures (1D nanowires) have been taken to inactivate bacteria. It has been confirmed that the electrical field near the tips of nanowires can be enhanced significantly (e.g. magnitude of 10^4) [287,288]. The enhanced electrical field builds intense dipole-dipole interactions with the lipid bilayer of the cell membrane, resulting in thinning of the membrane and finally electroporation pores immediately [287–292]. For example, Cui et al. reported that when applied with voltage of 20 V, silver nanowires could inactivate $> 98\%$ of bacteria within only a few seconds [288].

6. Toxicity of plasmonic nanomaterials

As discussed in above sections, plasmonic nanomaterials have demonstrated promising potentials for environmental remediation. However, the achievement in nanotechnology and the increasingly wide use of nanomaterials have raised concerns on their environmental impacts [293]. Specifically, the possibility of their release into environment and subsequent effects on the health of ecosystem is urgently necessary to be addressed [294]. The public debate on whether the environmental cost of nanotechnology outweigh its benefits has been growing [295].

6.1. Fate and transformation of plasmonic nanomaterials in the environment

Similar with many other engineered nanomaterials, gold and silver nanoparticles may be released into the environment during their whole life cycle, including the initial synthesis, the manufacturing and incorporation of nanomaterials into commercial products, the use of these products, and even the recycle and disposal of these products [296,297]. It should be noted that most engineered nanomaterials including gold and silver nanoparticles released from domestic and industrial sources enter sewer systems [298]. These nanoparticles then enter and transport among various environmental compartments, including surface waters, groundwater, soil, sediment, and even atmosphere [299] as follows (Fig. 9a): ① Nanomaterials in consumer products find their way through waste disposal streams and finally into wastewater treatment plants [300]; ② These nanomaterials can reach surface waters through wastewater effluents and ③ reach soils through the treatment of sludges, nanomaterial-based soil remediation [301], nanomaterials in fertilizers and plant-protective products can also directly enter soils [302]; ④ Nanomaterials can also enter groundwater through nano-enabled groundwater remediation technologies [296], and nanomaterials retained in soils can also break through soil matrix and reach groundwater [303]; ⑤ Nanomaterials in the soil may also enter surface waters through runoffs [304]; ⑥ Nanomaterials in surface waters undergo complex transformation and subsequent deposition to sediment [305]; ⑦ and ⑧ Nanomaterials that are emitted to ambient atmosphere can finally precipitate to surface waters and soils [303,306].

Gold and silver nanoparticles are then subject to transformations due to the complex conditions in these environmental compartments, and the transformations of silver are more complex than gold due to its more reactive chemistry. As a result, we mainly discuss the transformation of silver nanoparticles in the environment in this section. It is helpful to understand the physical and chemical processes in the synthesis of silver nanoparticles which is more simplified compared to the situations in the real environment. In a typical synthesis of silver nanoparticles, precursor of silver (usually silver salts), solvent, reducing agent (which reduce silver ions to silver atoms), and surfactant (which

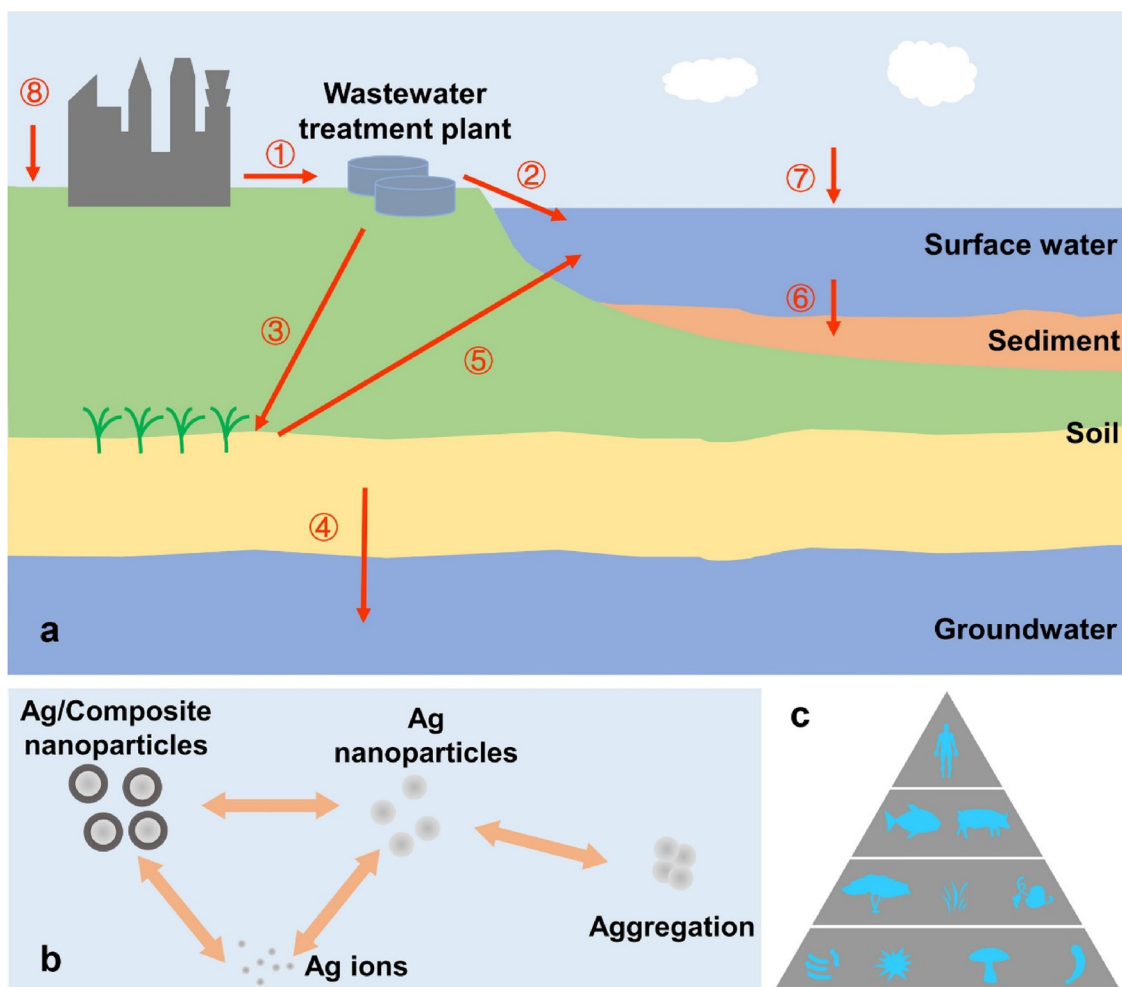


Fig. 9. (a) Nanomaterials enter the environmental compartments through several major routes. (b) Transformations of silver nanoparticles. (c) food web has been affected by plasmonic nanoparticles.

guide the growth of silver nanostructures and stabilize the nanoparticles, some surfactants can also serve as reducing agents) are mixed [307]. The produced silver atoms then organize into nanocrystals whose growth is significantly affected by the reaction conditions, such as temperature and types of solvent and surfactant. Because the reduction from silver ions to silver atoms and the dissolution from silver atoms to silver ions are dynamic, one can tune the reaction kinetics to control the structure of silver nanoparticles [308]. The silver nanoparticles are then collected by centrifugation. It should be noted that extensive centrifugation could result into the aggregation because the surfactants on the nanoparticles are removed under this condition. Even though there are enough surfactants on the surface of nanoparticles, they may undergo aggregation in the presence of high ionic strength [27]. It is also acceptable that the type of surfactants affects the aggregation of nanoparticles significantly. Because silver is relative reactive, silver nanoparticles can be oxidized and form a layer of Ag_2O on their surface during the storage [309]. Silver nanoparticle may also transform into Ag_2S [310] and silver halides [311] under certain reaction conditions.

Above processes (as simplified in Fig. 9b) are the fundamentals of the transformations of silver nanoparticles in the real environment. The difference between the situations in the real environment and in the batch studies in the laboratory is that the affecting parameters in the environment are significantly more and the chemistry is more complex. For example, the ionic strength for seawater can be as high as 700 mM, which is enough to induce the aggregation of silver nanoparticles

[312]. Meanwhile, the halides in seawater could also transform silver to silver halides [178]. Another key component in environmental compartments is natural organic matter (NOM), which can potentially replace the surfactants on the surface of nanoparticles (this process is similar to the ligand exchange mechanism in the colloidal chemistry), and thus affect their transformations [313]. Because of the complex nature of NOM, they can either increase the stability of silver nanoparticles, or facilitate their dissolution [314–319]. On the other hand, the sulfidation of silver to Ag_2S nanoparticles was widely observed in wastewaters possibly due to the relatively high concentration of H_2S [300]. It should also be noted that the formation of different silver compounds (e.g. Ag_2O , Ag_2S , and silver halides) can greatly affect the release of silver ions since these compounds have different dissolution rates compared to pristine silver nanoparticles [312]. Recent studies also show that the chemistry at the interface between inorganic nanoparticles and organisms can affect the transformation of gold nanoparticles [320,321].

6.2. Toxicity of plasmonic nanomaterials in the environment

Due to the complicated fate and transformations of plasmonic nanomaterials in the environment, all the relevant organisms may be affected since the nanomaterials in compartments can transport to food webs [322]. Numerous studies have reported the possible toxicity of plasmonic nanoparticles to food web numbers (Fig. 9c). For example, as we have discussed in Section 4, plasmonic nanomaterials are able to

inactivate bacteria. Besides the toxicity revealed by disinfection applications, silver nanoparticles have been verified to affect natural bacterial communities in sewage sludge [323,324], in sediment [325], and in soil [315]. A previous study evidenced the possibly adverse effect of gold nanoparticles on reproduction of earthworm, and suggested the nanoparticles in soil may enter terrestrial food webs [326]. Plasmonic nanoparticles can also adhere to the exoskeleton of invertebrates to form aggregation and cause toxicity [327], which can be significantly affected by NOM [318]. Silver and gold nanoparticles also have shown the effects on the growth, biochemical traits, and production of plants [301,328–331]. *In vivo* and *in vitro* assessment has shown the adverse effect of gold and silver nanoparticles on animals [332,333]. Studies on the cellular level also suggest the possible effects of plasmonic nanoparticles on human health [334,335]. However, we noted that few studies have focused on food web research [322,336] and long-term toxicity of plasmonic nanomaterials.

The inactivation effects of silver nanoparticles on bacteria, which has been discussed in Section 4, is mainly attributed to the release of silver ions and the generation of ROS (Fig. 8). However, toxicological studies sometimes present controversial results on the origin of the toxicity of silver nanoparticles [333]. Whether the toxicity of silver nanoparticles is from the nanoparticles themselves or the silver ions released by them is still an undergoing debate. A previous study revealed that the ratio between silver nanoparticles and silver ions in the suspension of silver nanoparticles is critical to the results [337]. However, from the perspective of colloidal chemistry, the release rate of silver ions from silver nanoparticles is highly dependent on the size, morphology, surfactant, composition, and the ambient environment of silver nanoparticles. Meanwhile, these factors also affect the transformation of silver nanoparticles. It is thus challenging to isolate the effects from the silver nanoparticles themselves and silver ions on the toxicological performance.

Different from silver, bulk gold is considered to be “safe” and chemically inert. However, beside the antibacterial properties induced by photothermal therapy, gold nanoparticles are also of toxicological properties. One of the mechanisms is the surfactants used for the synthesis of gold nanoparticles are sometimes toxic. For example, cetyltrimethylammonium bromide (CTAB, a toxic chemical) is often used for the synthesis of gold nanorods to direct the particle growth in one direction [49], which may be released to the ambient environment from inadequate purification or desorption of surfactant from the surface of the nanorods and induce toxicity [334]. Size effect also plays an important role for the toxicity of gold nanoparticles. It has been shown that gold nanoparticles below certain sizes are able to pass the membrane of cells, and because the gold nanoparticles with smaller size are more active and able to produce ROS, they can induce toxicity.

7. Summary and outlook

The recent progress of the environmental applications plasmonic (nano) materials and their underlying mechanisms has been evaluated. Many efforts have been devoted to the remediation of contaminants in water and air with plasmonic nanomaterials due to their fantastic properties, including tunable optical properties, significant photothermal effect, satisfactory electrical conductivity, and excellent catalytic activity. Various studies have shown that not only conventional contaminants (e.g. dyes), but also many emerging contaminants such as pharmaceuticals and personal care products and endocrine disrupting chemicals in water can be decomposed by using plasmonic photocatalysis. Plasmonic nanomaterials have also been intensively studied to address the air pollution issues such as VOCs and flue gases. The inactivation of bacteria with plasmonic nanomaterials is another field of interest. The following issues should also be considered while selecting nanomaterials for photocatalytic applications.

- (1) complete mineralization of contaminants must be achieved in some cases due to the potential risks of intermediates;
- (2) the cost of plasmonic nanomaterials and the associated treatment processes need to be significantly decreased.

It is reasonable to consider that plasmonic nanomaterials may not be used for the removal of all types of organics at least based on cost, since most plasmonic metals are noble except copper. However, plasmonic nanomaterials may be promising for the control of trace contaminants, which are of high concern and difficult to be removed by conventional treatment processes. Meanwhile, the recyclability and stability of plasmonic nanomaterials are also two parameters to further lower the cost of this technology;

- (3) How to improve the stability of plasmonic nanomaterials in real environmental matrices is essentially important for their practical use. Most of current studies have focused on the performance test in synthetic waters, but few of them considered the interaction between complex water components with functional nanomaterials. Moreover, the potentially ecological risks of these materials should be investigated in case of failed recycle or recovery.
- (4) The ecological safety of plasmonic nanomaterials certainly has a significant effect on their applications. Even though no simple conclusions from previous studies can be drawn due to the different experimental designs, it is clearly shown that plasmonic nanomaterials can affect the ecosystem. It is thus highly important to evaluate the applications of plasmonic nanomaterials from a life-cycle perspective. Meanwhile, more sustainable synthesis of plasmonic nanomaterials and their integration in devices are also desirable.

Beyond the progress summarized here, we also find some other opportunities for plasmonic nanotechnologies in the environmental sector. Few examples are summarized here: (i) Wastewater is now being considered as a valuable resource other than waste, so how to recycle the nutrients, heavy metals, and energy from wastewater is of high interest; (ii) In addition to plasmonic nanomaterials, most of the other functional nanomaterials are designed for the remediation of water and air pollution, while only few of them are used in soil decontamination. However, soil decontamination has gained intensive attention recently since many heavy metals and toxic organics have been found in soils. How to address the issue of soil contamination is another critical question; (iii) In addition, plasmonic nanomaterials are promising for the detection of various contaminants, including organic and inorganic pollutants as well as pathogenic microorganisms. (iv) One can certainly design an appropriate device for detection purposes, but for remediation purposes, especially water treatment, we should consider carefully on how to assemble nanotechnology into conventional water treatment processes. The debate on whether photocatalysis is a pretreatment or a post-treatment process is still ongoing and is based on the properties of the treated water. However, regardless of the outcome of the debate, proper design of photocatalytic reactors to improve the photocatalytic efficiency is of high interest.

Acknowledgements

This study was supported by the National Natural Science Foundation of China (No. 91547105 and 51779076); the Foundation for Innovative Research Groups of the National Natural Science Foundation of China (No. 51421006); the Priority Academic Program Development of Jiangsu Higher Education Institutions (PAPD); the Six Talent Peaks Project of Jiangsu Province (2016-JNHB 007); the 333 Talent Project Foundation of Jiangsu Province. D.D. Dionysiou also acknowledges support from the University of Cincinnati through a UNESCO co-Chair Professor position on “Water Access and Sustainability” and the Herman Schneider Professorship in the College of Engineering and Applied Sciences.

References

[1] L. Rodríguez-Lado, G. Sun, M. Berg, Q. Zhang, H. Xue, Q. Zheng, C.A. Johnson, Groundwater arsenic contamination throughout China, *Science* 341 (2013) 866–868.

[2] R.B. Johnston, S. Hanchett, M.H. Khan, The socio-economics of arsenic removal, *Nat. Geosci.* 3 (2010) 2–3.

[3] D. Wang, Y. Li, W. Zhang, Q. Wang, P. Wang, C. Wang, Development and modeling of a flat plate serpentine reactor for photocatalytic degradation of 17-ethynyles-tradiol, *Environ. Sci. Pollut. Res.* 20 (2013) 2321–2329.

[4] Arsenic in Groundwater of the United States, (2011).

[5] P.V. Kamat, Meeting the clean energy demand: nanostructure architectures for solar energy conversion, *J. Phys. Chem. C* 111 (2007) 2834–2860.

[6] P.V. Kamat, Quantum dot solar cells. Semiconductor nanocrystals as light harvesters, *J. Phys. Chem. C* 112 (2008) 18737–18753.

[7] U.G. Akpan, B.H. Hameed, Parameters affecting the photocatalytic degradation of dyes using TiO_2 -based photocatalysts: a review, *J. Hazard. Mater.* 170 (2009) 520–529.

[8] C. Byrne, G. Subramanian, S.C. Pillai, Recent advances in photocatalysis for environmental applications, *J. Environ. Chem. Eng.* (2017).

[9] A.J. Ebele, M. Abou-Elwafa Abdallah, S. Harrad, Pharmaceuticals and personal care products (PPCPs) in the freshwater aquatic environment, *Emerg. Contam.* 3 (2017) 1–16.

[10] R. Fagan, D.E. McCormack, D.D. Dionysiou, S.C. Pillai, A review of solar and visible light active TiO_2 photocatalysis for treating bacteria, cyanotoxins and contaminants of emerging concern, *Mater. Sci. Semicond. Process.* 42 (Part 1) (2016) 2–14.

[11] P.G. Tratnyek, R.L. Johnson, Nanotechnologies for environmental cleanup, *Nano Today* 1 (2006) 44–48.

[12] X. Quan, S. Yang, X. Ruan, H. Zhao, Preparation of titania nanotubes and their environmental applications as electrode, *Environ. Sci. Technol.* 39 (2005) 3770–3775.

[13] J. Yuan, X. Liu, O. Akbulut, J. Hu, S.L. Suib, J. Kong, F. Stellacci, Superwetting nanowire membranes for selective absorption, *Nat. Nano* 3 (2008) 332–336.

[14] Z. Ai, W. Ho, S. Lee, L. Zhang, Efficient photocatalytic removal of NO in indoor air with hierarchical bismuth oxybromide nanoplate microspheres under visible light, *Environ. Sci. Technol.* 43 (2009) 4143–4150.

[15] R. Wang, K. Hashimoto, A. Fujishima, M. Chikuni, E. Kojima, A. Kitamura, M. Shimohigoshi, T. Watanabe, Light-induced amphiphilic surfaces, *Nature* 388 (1997) 431–432.

[16] S. Banerjee, D.D. Dionysiou, S.C. Pillai, Self-cleaning applications of TiO_2 by photo-induced hydrophilicity and photocatalysis, *Appl. Catal. B: Environ.* 176–177 (2015) 396–428.

[17] M.L. Brongersma, V.M. Shalaev, The case for plasmonics, *Science* 328 (2010) 440–441.

[18] M. Ryeng, C.M. Cobley, J. Zeng, W. Li, C.H. Moran, Q. Zhang, D. Qin, Y. Xia, Controlling the synthesis and assembly of silver nanostructures for plasmonic applications, *Chem. Rev.* 111 (2011) 3669–3712.

[19] N.J. Halas, S. Lal, W.-S. Chang, S. Link, P. Nordlander, Plasmons in strongly coupled metallic nanostructures, *Chem. Rev.* 111 (2011) 3913–3961.

[20] G.V. Hartland, Optical studies of dynamics in noble metal nanostructures, *Chem. Rev.* 111 (2011) 3858–3887.

[21] S. Lal, S. Link, N.J. Halas, Nano-optics from sensing to waveguiding, *Nat. Photon.* 1 (2007) 641–648.

[22] E. Hutter, J.H. Fendler, Exploitation of localized surface plasmon resonance, *Adv. Mater.* 16 (2004) 1685–1706.

[23] W.A. Murray, W.L. Barnes, Plasmonic materials, *Adv. Mater.* 19 (2007) 3771–3782.

[24] M.-C. Daniel, D. Astruc, Gold nanoparticles: assembly, supramolecular chemistry, quantum-size-related properties, and applications toward biology, catalysis, and nanotechnology, *Chem. Rev.* 104 (2004) 293–346.

[25] X. Liu, M.T. Swihart, Heavily-doped colloidal semiconductor and metal oxide nanocrystals: an emerging new class of plasmonic nanomaterials, *Chem. Soc. Rev.* 43 (2014) 3908–3920.

[26] M. Hu, J. Chen, Z.-Y. Li, L. Au, G.V. Hartland, X. Li, M. Marquez, Y. Xia, Gold nanostructures: engineering their plasmonic properties for biomedical applications, *Chem. Soc. Rev.* 35 (2006) 1084–1094.

[27] X. Han, J. Goebel, Z. Lu, Y. Yin, Role of salt in the spontaneous assembly of charged gold nanoparticles in ethanol, *Langmuir* 27 (2011) 5282–5289.

[28] Q. Zhang, W. Li, C. Moran, J. Zeng, J. Chen, L.-P. Wen, Y. Xia, Seed-mediated synthesis of Ag nanocubes with controllable edge lengths in the range of 30–200 nm and comparison of their optical properties, *J. Am. Chem. Soc.* 132 (2010) 11372–11378.

[29] C. Gao, Y. Hu, M. Wang, M. Chi, Y. Yin, Fully alloyed Ag/Au nanospheres: combining the plasmonic property of Ag with the stability of Au, *J. Am. Chem. Soc.* 136 (2014) 7474–7479.

[30] X. Huang, S. Li, Y. Huang, S. Wu, X. Zhou, S. Li, C.L. Gan, F. Boey, C.A. Mirkin, H. Zhang, Synthesis of hexagonal close-packed gold nanostructures, *Nat. Commun.* 2 (2011) 292.

[31] X. Lu, M.S. Yavuz, H.-Y. Tuan, B.A. Korgel, Y. Xia, Ultrathin gold nanowires can be obtained by reducing polymeric strands of oleylamine–AuCl complexes formed via aurophilic interaction, *J. Am. Chem. Soc.* 130 (2008) 8900–8901.

[32] T.K. Sau, C.J. Murphy, Seeded high yield synthesis of short Au nanorods in aqueous solution, *Langmuir* 20 (2004) 6414–6420.

[33] Z. Zheng, T. Tachikawa, T. Majima, Single-particle study of Pt-modified Au nanorods for plasmon-enhanced hydrogen generation in visible to near-infrared region, *J. Am. Chem. Soc.* 136 (2014) 6870–6873.

[34] J. Henzie, M. Grünewald, A. Widmer-Cooper, P.L. Geissler, P. Yang, Self-assembly of uniform polyhedral silver nanocrystals into densest packings and exotic superlattices, *Nat. Mater.* 11 (2012) 131–137.

[35] L. Chen, F. Ji, Y. Xu, L. He, Y. Mi, F. Bao, B. Sun, X. Zhang, Q. Zhang, High-yield seedless synthesis of triangular gold nanoplates through oxidative etching, *Nano Lett.* 14 (2014) 7201–7206.

[36] A. Gao, W. Xu, Y. Ponce de León, Y. Bai, M. Gong, K. Xie, B.H. Park, Y. Yin, Controllable fabrication of Au nanocups by confined-space thermal dewetting for OCT imaging, *Adv. Mater.* 29 (2017) 1701070–n/a.

[37] K. Liu, Y. Bai, L. Zhang, Z. Yang, Q. Fan, H. Zheng, Y. Yin, C. Gao, Porous Au–Ag nanospheres with high-density and highly accessible hotspots for SERS analysis, *Nano Lett.* 16 (2016) 3675–3681.

[38] Y. Sun, Y. Xia, Mechanistic study on the replacement reaction between silver nanostructures and chloroauric acid in aqueous medium, *J. Am. Chem. Soc.* 126 (2004) 3892–3901.

[39] Q. Lu, A.-L. Wang, Y. Gong, W. Hao, H. Cheng, J. Chen, B. Li, N. Yang, W. Niu, J. Wang, Y. Yu, X. Zhang, Y. Chen, Z. Fan, X.-J. Wu, J. Chen, J. Luo, S. Li, L. Gu, H. Zhang, Crystal phase-based epitaxial growth of hybrid noble metal nanostructures on 4H/4c fcc Au nanowires, *Nat. Chem.* 10 (2018) 456–461.

[40] H.-E. Lee, H.-Y. Ahn, J. Mun, Y.Y. Lee, M. Kim, N.H. Cho, K. Chang, W.S. Kim, J. Rho, K.T. Nam, Amino-acid- and peptide-directed synthesis of chiral plasmonic gold nanoparticles, *Nature* 556 (2018) 360–365.

[41] M. Nakagawa, T. Kawai, Chirality-controlled syntheses of double-helical Au nanowires, *J. Am. Chem. Soc.* 140 (2018) 4991–4994.

[42] E. González, J. Arbiol, V.F. Puntes, Carving at the nanoscale: sequential galvanic exchange and Kirkendall growth at room temperature, *Science* 334 (2011) 1377–1380.

[43] G.A. López-Muñoz, J.A. Pescador-Rojas, J. Ortega-López, J.S. Salazar, J.A. Balderas-López, Thermal diffusivity measurement of spherical gold nanofluids of different sizes/concentrations, *Nanoscale Res. Lett.* 7 (2012) 423.

[44] K.-S. Lee, M.A. El-Sayed, Dependence of the enhanced optical scattering efficiency relative to that of absorption for gold metal nanorods on aspect ratio, size, end-cap shape, and medium refractive index, *J. Phys. Chem. B* 109 (2005) 20331–20338.

[45] L. Zhang, D.A. Blom, H. Wang, Au– Cu_2O core–shell nanoparticles: a hybrid metal–semiconductor heteronanostructure with geometrically tunable optical properties, *Chem. Mater.* 23 (2011) 4587–4598.

[46] Y. Lu, Y. Yin, B.T. Mayers, Y. Xia, Modifying the surface properties of superparamagnetic iron oxide nanoparticles through a sol–gel approach, *Nano Lett.* 2 (2002) 183–186.

[47] Z.W. Seh, S. Liu, M. Low, S.-Y. Zhang, Z. Liu, A. Mlayah, M.-Y. Han, Janus Au– TiO_2 photocatalysts with strong localization of plasmonic near-fields for efficient visible-light hydrogen generation, *Adv. Mater.* 24 (2012) 2310–2314.

[48] C. Gao, J. Vuong, Q. Zhang, Y. Liu, Y. Yin, One-step seeded growth of Au nanoparticles with widely tunable sizes, *Nanoscale* 4 (2012) 2875–2878.

[49] B. Nikoobakh, M.A. El-Sayed, Preparation and growth mechanism of gold nanorods (NRs) using seed-mediated growth method, *Chem. Mater.* 15 (2003) 1957–1962.

[50] H. Chen, L. Shao, Q. Li, J. Wang, Gold nanorods and their plasmonic properties, *Chem. Soc. Rev.* 42 (2013) 2679–2724.

[51] P.K. Jain, M.A. El-Sayed, Plasmonic coupling in noble metal nanostructures, *Chem. Phys. Lett.* 487 (2010) 153–164.

[52] Y. Liu, X. Han, L. He, Y. Yin, Thermoresponsive assembly of charged gold nanoparticles and their reversible tuning of plasmon coupling, *Angew. Chem. Int. Ed.* 51 (2012) 6373–6377.

[53] Z. Sun, W. Ni, Z. Yang, X. Kou, L. Li, J. Wang, pH-controlled reversible assembly and disassembly of gold nanorods, *Small* 4 (2008) 1287–1292.

[54] Q. Zhang, J. Ge, T. Pham, J. Goebel, Y. Hu, Z. Lu, Y. Yin, Reconstruction of silver nanoplates by UV irradiation: tailored optical properties and enhanced stability, *Angew. Chem. Int. Ed.* 48 (2009) 3516–3519.

[55] Y. Yang, J. Liu, Z.W. Fu, D. Qin, Galvanic replacement-free deposition of Au on Ag for core–shell nanocubes with enhanced chemical stability and SERS activity, *J. Am. Chem. Soc.* 136 (2014) 8153–8156.

[56] S. Link, C. Burda, B. Nikoobakh, M.A. El-Sayed, Laser-induced shape changes of colloidal gold nanorods using femtosecond and nanosecond laser pulses, *J. Phys. Chem. B* 104 (2000) 6152–6163.

[57] J. Qiu, W.D. Wei, Surface plasmon-mediated photothermal chemistry, *J. Phys. Chem. C* 118 (2014) 20735–20749.

[58] G. González-Rubio, P. Díaz-Núñez, A. Rivera, A. Prada, G. Tardajos, J. González-Izquierdo, L. Bañares, P. Llombart, L.G. Macdowell, M. Alcolea Palafox, L.M. Liz-Marzán, O. Peña-Rodríguez, A. Guerrero-Martínez, Femtosecond laser reshaping yields gold nanorods with ultranarrow surface plasmon resonances, *Science* 358 (2017) 640–644.

[59] G. Baffou, R. Quidant, C. Girard, Heat generation in plasmonic nanostructures: influence of morphology, *Appl. Phys. Lett.* 94 (2009) 153109.

[60] A.O. Govorov, H.H. Richardson, Generating heat with metal nanoparticles, *Nano Today* 2 (2007) 30–38.

[61] X. Chen, Y. Chen, M. Yan, M. Qiu, Nanosecond photothermal effects in plasmonic nanostructures, *ACS Nano* 6 (2012) 2550–2557.

[62] F. Wang, C. Li, H. Chen, R. Jiang, L.-D. Sun, Q. Li, J. Wang, G.-C. Yu, C.-H. Yan,

Plasmonic harvesting of light energy for Suzuki coupling reactions, *J. Am. Chem. Soc.* 135 (2013) 5588–5601.

[63] X. Wang, M. Zhu, Y. Sun, W. Fu, Q. Gu, C. Zhang, Y. Zhang, Y. Dai, Y. Sun, A new insight of the photothermal effect on the highly efficient visible-light-driven photocatalytic performance of novel-designed TiO_2 rambutan-like microspheres decorated by Au nanorods, *Part. Part. Syst. Char.* 33 (2016) 140–149.

[64] P.C. Ray, S.A. Khan, A.K. Singh, D. Senapati, Z. Fan, Nanomaterials for targeted detection and photothermal killing of bacteria, *Chem. Soc. Rev.* 41 (2012) 3193–3209.

[65] O. Neumann, A.S. Urban, J. Day, S. Lal, P. Nordlander, N.J. Halas, Solar vapor generation enabled by nanoparticles, *ACS Nano* 7 (2013) 42–49.

[66] R.A. Serway, *Principles of Physics*, 2nd ed., Saundier College Pub., London, 1998.

[67] T. Tatsuma, H. Nishi, T. Ishida, Plasmon-induced charge separation: chemistry and wide applications, *Chem. Sci.* 8 (2017) 3325–3337.

[68] C.G. Freysschlag, R.J. Madix, Precious metal magic: catalytic wizardry, *Mater. Today* 14 (2011) 134–142.

[69] P. Christopher, H. Xin, S. Linic, Visible-light-enhanced catalytic oxidation reactions on plasmonic silver nanostructures, *Nat. Chem.* 3 (2011) 467–472.

[70] S. Linic, P. Christopher, D.B. Ingram, Plasmonic-metal nanostructures for efficient conversion of solar to chemical energy, *Nat. Mater.* 10 (2011) 911–921.

[71] H.A. Atwater, A. Polman, Plasmonics for improved photovoltaic devices, *Nat. Mater.* 9 (2010) 205–213.

[72] H. Tong, S. Ouyang, Y. Bi, N. Umezawa, M. Oshikiri, J. Ye, Nano-photocatalytic materials: possibilities and challenges, *Adv. Mater.* 24 (2012) 229–251.

[73] M.R. Hoffmann, S.T. Martin, W. Choi, D.W. Bahnemann, Environmental applications of semiconductor photocatalysis, *Chem. Rev.* 95 (1995) 69–96.

[74] G.A. Olah, G.K.S. Prakash, A. Goeppert, Anthropogenic chemical carbon cycle for a sustainable future, *J. Am. Chem. Soc.* 133 (2011) 12881–12898.

[75] T. Wu, G. Liu, J. Zhao, H. Hidaka, N. Serpone, Photoassisted degradation of dye pollutants. V. Self-photosensitized oxidative transformation of rhodamine B under visible light irradiation in aqueous TiO_2 dispersions, *J. Phys. Chem. B* 102 (1998) 5845–5851.

[76] L. Liu, S. Ouyang, J. Ye, Gold-nanorod-photosensitized titanium dioxide with wide-range visible-light harvesting based on localized surface plasmon resonance, *Angew. Chem. Int. Ed.* 52 (2013) 6689–6693.

[77] K. Sayama, H. Arakawa, Effect of carbonate salt addition on the photocatalytic decomposition of liquid water over Pt- TiO_2 catalyst, *Journal of the Chemical Society, Faraday Trans.* 93 (1997) 1647–1654.

[78] G.L. Chiarello, E. Sell, L. Forni, Photocatalytic hydrogen production over flame spray pyrolysis-synthesised TiO_2 and Au/ TiO_2 , *Appl. Catal. B: Environ.* 84 (2008) 332–339.

[79] E. Bae, W. Choi, Highly enhanced photoreductive degradation of perchlorinated compounds on dye-sensitized metal/ TiO_2 under visible light, *Environ. Sci. Technol.* 37 (2003) 147–152.

[80] I.M. Arabatzis, T. Stergiopoulos, D. Andreeva, S. Kitova, S.G. Neophytides, P. Falaras, Characterization and photocatalytic activity of Au/ TiO_2 thin films for azo-dye degradation, *J. Catal.* 220 (2003) 127–135.

[81] D. Ke, T. Peng, L. Ma, P. Cai, P. Jiang, Photocatalytic water splitting for O_2 production under visible-light irradiation on $BiVO_4$ nanoparticles in different sacrificial reagent solutions, *Appl. Catal. A* 350 (2008) 111–117.

[82] R. Georgekutty, M.K. Seery, S.C. Pillai, A highly efficient Ag-ZnO photocatalyst: synthesis, properties, and mechanism, *J. Phys. Chem. C* 112 (2008) 13563–13570.

[83] W. Lu, S. Gao, J. Wang, One-pot synthesis of Ag/ZnO self-assembled 3D hollow microspheres with enhanced photocatalytic performance, *J. Phys. Chem. C* 112 (2008) 16792–16800.

[84] S. Anandan, P. Sathish Kumar, N. Pugazhenthiran, J. Madhavan, P. Maruthamuthu, Effect of loaded silver nanoparticles on TiO_2 for photocatalytic degradation of Acid Red 88, *Sol. Energy Mater. Sol. C* 92 (2008) 929–937.

[85] X.-G. Hou, M.-D. Huang, X.-L. Wu, A.-D. Liu, Preparation and studies of photocatalytic silver-loaded TiO_2 films by hybrid sol-gel method, *Chem. Eng. J.* 146 (2009) 42–48.

[86] T. Hirakawa, P.V. Kamat, Charge separation and catalytic activity of Ag@ TiO_2 core-shell composite clusters under UV-irradiation, *J. Am. Chem. Soc.* 127 (2005) 3928–3934.

[87] A. Takai, P.V. Kamat, Capture, Store, and discharge. Shuttling photogenerated electrons across TiO_2 -silver interface, *ACS Nano* 5 (2011) 7369–7376.

[88] Y. Tian, T. Tatsuma, Mechanisms and applications of plasmon-induced charge separation at TiO_2 films loaded with gold nanoparticles, *J. Am. Chem. Soc.* 127 (2005) 7632–7637.

[89] A.J. Bard, Design of semiconductor photoelectrochemical systems for solar energy conversion, *J. Phys. Chem.* 86 (1982) 172–177.

[90] L. de la Garza, G. Jeong, P.A. Liddell, T. Sotomura, T.A. Moore, A.L. Moore, D. Gust, Enzyme-based photoelectrochemical biofuel cell, *J. Phys. Chem. B* 107 (2003) 10252–10260.

[91] Y.K. Lee, C.H. Jung, J. Park, H. Seo, G.A. Somorjai, J.Y. Park, Surface plasmon-driven hot electron flow probed with metal-semiconductor nanodiodes, *Nano Lett.* 11 (2011) 4251–4255.

[92] Y. Tang, Z. Jiang, G. Xing, A. Li, P.D. Kanhere, Y. Zhang, T.C. Sum, S. Li, X. Chen, Z. Dong, Z. Chen, Efficient Ag@AgCl cubic cage photocatalysts profit from ultra-fast plasmon-induced electron transfer processes, *Adv. Funct. Mater.* 23 (2013) 2932–2940.

[93] J.S. DuChene, B.C. Sweeny, A.C. Johnston-Peck, D. Su, E.A. Stach, W.D. Wei, Prolonged hot electron dynamics in plasmonic-metal/semiconductor heterostructures with implications for solar photocatalysis, *Angew. Chem. Int. Ed.* 53 (2014) 7887–7891.

[94] A.O. Govorov, H. Zhang, Y.K. Gun'ko, Theory of photo-injection of hot plasmonic carriers from metal nanostructures into semiconductors and surface molecules, *J. Phys. Chem. C* 117 (2013) 16616–16631.

[95] S. Mubeen, G. Hernandez-Sosa, D. Moses, J. Lee, M. Moskovits, Plasmonic photo-sensitization of a wide band gap semiconductor: converting plasmons to charge carriers, *Nano Lett.* 11 (2011) 5548–5552.

[96] W.A. Tisdale, K.J. Williams, B.A. Timp, D.J. Norris, E.S. Aydil, X.-Y. Zhu, Hot-electron transfer from semiconductor nanocrystals, *Science* 328 (2010) 1543–1547.

[97] L.V. Besteiro, X.-T. Kong, Z. Wang, G. Hartland, A.O. Govorov, Understanding hot-electron generation and plasmon relaxation in metal nanocrystals: quantum and classical mechanisms, *ACS Nano* 4 (2017) 2759–2781.

[98] J.B. Priebe, M. Karnahl, H. Junge, M. Beller, D. Hollmann, A. Brückner, Water reduction with visible light: synergy between optical transitions and electron transfer in Au- TiO_2 catalysts visualized by in situ EPR spectroscopy, *Angew. Chem. Int. Ed.* 52 (2013) 11420–11424.

[99] C. Gomes Silva, R. Juárez, T. Marino, R. Molinari, H. García, Influence of excitation wavelength (UV or visible light) on the photocatalytic activity of titania containing gold nanoparticles for the generation of hydrogen or oxygen from Water, *J. Am. Chem. Soc.* 133 (2011) 595–602.

[100] K. Qian, B.C. Sweeny, A.C. Johnston-Peck, W. Niu, J.O. Graham, J.S. DuChene, J. Qiu, Y.-C. Wang, M.H. Engelhard, D. Su, E.A. Stach, W.D. Wei, Surface plasmon-driven water reduction: gold nanoparticle size matters, *J. Am. Chem. Soc.* 136 (2014) 9842–9845.

[101] J. Lee, S. Mubeen, X. Ji, G.D. Stucky, M. Moskovits, Plasmonic photoanodes for solar water splitting with visible light, *Nano Lett.* 12 (2012) 5014–5019.

[102] X. Zhang, Y. Liu, S.-T. Lee, S. Yang, Z. Kang, Coupling surface plasmon resonance of gold nanoparticles with slow-photon-effect of TiO_2 photonic crystals for synergistically enhanced photoelectrochemical water splitting, *Energy Environ. Sci.* 7 (2014) 1409–1419.

[103] A. Paracchino, V. Laporte, K. Sivula, M. Grätzel, E. Thimsen, Highly active oxide photocathode for photoelectrochemical water reduction, *Nat. Mater.* 10 (2011) 456–461.

[104] E. Thimsen, F. Le Formal, M. Grätzel, S.C. Warren, Influence of plasmonic Au nanoparticles on the photoactivity of Fe_2O_3 electrodes for water splitting, *Nano Lett.* 11 (2011) 35–43.

[105] A. Primo, T. Marino, A. Corma, R. Molinari, H. García, Efficient visible-light photocatalytic water splitting by minute amounts of gold supported on nanoparticulate CeO_2 obtained by a biopolymer templating method, *J. Am. Chem. Soc.* 133 (2011) 6930–6933.

[106] H. Lin, L. Ding, Z. Pei, Y. Zhou, J. Long, W. Deng, X. Wang, Au deposited $BiOCl$ with different facets: on determination of the facet-induced transfer preference of charge carriers and the different plasmonic activity, *Appl. Catal. B: Environ.* 160–161 (2014) 98–105.

[107] V. Subramanian, E.E. Wolf, P.V. Kamat, Catalysis with TiO_2 /gold nanocomposites. Effect of metal particle size on the fermi level equilibration, *J. Am. Chem. Soc.* 126 (2004) 4943–4950.

[108] E. Kowalska, O.O.P. Mahaney, R. Abe, B. Ohtani, Visible-light-induced photocatalysis through surface plasmon excitation of gold on titania surfaces, *Phys. Chem. Chem. Phys.* 12 (2010) 2344–2355.

[109] B. Ohtani, Photocatalysis A to Z—what we know and what we do not know in A scientific sense, *J. Photochem. Photobiol. C: Photochem. Rev.* 11 (2010) 157–178.

[110] E. Kowalska, R. Abe, B. Ohtani, Visible-light-induced photocatalytic reaction of gold-modified titanium(iv) oxide particles: action spectrum analysis, *Chem. Commun.* (2009) 241–243.

[111] D.B. Ingram, S. Linic, Water splitting on composite plasmonic-metal/semiconductor photoelectrodes: evidence for selective plasmon-induced formation of charge carriers near the semiconductor surface, *J. Am. Chem. Soc.* 133 (2011) 5202–5205.

[112] S.D. Standridge, G.C. Schatz, J.T. Hupp, Distance dependence of plasmon-enhanced photocurrent in dye-sensitized solar cells, *J. Am. Chem. Soc.* 131 (2009) 8407–8409.

[113] J. Tang, Z. Huo, S. Brittman, H. Gao, P. Yang, Solution-processed core-shell nanowires for efficient photovoltaic cells, *Nat. Nano* 6 (2011) 568–572.

[114] K. Maeda, K. Teramura, D. Lu, N. Saito, Y. Inoue, K. Domen, Noble-metal/ Cr_2O_3 core/shell nanoparticles as a cocatalyst for photocatalytic overall water splitting, *Angew. Chem. Int. Ed.* 45 (2006) 7806–7809.

[115] N. Sakamoto, H. Ohtsuka, T. Ikeda, K. Maeda, D. Lu, M. Kanehara, K. Teramura, T. Teranishi, K. Domen, Highly dispersed noble-metal/chromia (core/shell) nanoparticles as efficient hydrogen evolution promoters for photocatalytic overall water splitting under visible light, *Nanoscale* 1 (2009) 106–109.

[116] M. Yoshida, K. Takanabe, K. Maeda, A. Ishikawa, J. Kubota, Y. Sakata, Y. Ikezawa, K. Domen, Role and function of noble-metal/Cr-layer core/shell structure cocatalysts for photocatalytic overall water splitting studied by model electrodes, *J. Phys. Chem. C* 113 (2009) 10151–10157.

[117] K. Maeda, K. Teramura, D. Lu, N. Saito, Y. Inoue, K. Domen, Roles of Rh/ Cr_2O_3 (core/shell) nanoparticles photodeposited on visible-light-responsive ($Ga_{1-x}Zn_x$) ($Ni_{1-x}O_x$) solid solutions in photocatalytic overall water splitting, *J. Phys. Chem. C* 111 (2007) 7554–7560.

[118] K. Awazu, M. Fujimaki, C. Rockstuhl, J. Tominaga, H. Murakami, Y. Ohki, N. Yoshida, T. Watanabe, A plasmonic photocatalyst consisting of silver

nanoparticles embedded in titanium dioxide, *J. Am. Chem. Soc.* 130 (2008) 1676–1680.

[119] D. Wang, Z. Li, J. Zhou, H. Fang, X. He, P. Jena, J.-B. Zeng, W.-N. Wang, Simultaneous detection and removal of formaldehyde at room temperature: Janus Au@ZnO@ZIF-8 nanoparticles, *Nano-Micro Lett.* 10 (2017) 4.

[120] S.K. Cushing, J. Li, F. Meng, T.R. Senty, S. Suri, M. Zhi, M. Li, A.D. Bristow, N. Wu, Photocatalytic activity enhanced by plasmonic resonant energy transfer from metal to semiconductor, *J. Am. Chem. Soc.* 134 (2012) 15033–15041.

[121] X. Hu, X. Zhou, R. Wang, C. Hu, J. Qu, Characterization and photostability of Cu₂O–Ag–AgBr/Al₂O₃ for the degradation of toxic pollutants with visible-light irradiation, *Appl. Catal. B: Environ.* 154–155 (2014) 44–50.

[122] J. Zhang, Z. Zhu, Y. Tang, K. Müllen, X. Feng, Titania nanosheet-mediated construction of a two-dimensional titania/cadmium sulfide heterostructure for high hydrogen evolution activity, *Adv. Mater.* 26 (2014) 734–738.

[123] L. Sun, W. Wu, S. Yang, J. Zhou, M. Hong, X. Xiao, F. Ren, C. Jiang, Template and silica interlayer tailororable synthesis of spindle-like multilayer α-Fe₂O₃/Ag/SnO₂ ternary hybrid architectures and their enhanced photocatalytic activity, *ACS Appl. Mater. Interfaces* 6 (2014) 1113–1124.

[124] X. Yu, A. Shavel, X. An, Z. Luo, M. Ibáñez, A. Cabot, Cu₂ZnSnS₄–Pt and Cu₂ZnSnS₄–Au heterostructured nanoparticles for photocatalytic water splitting and pollutant degradation, *J. Am. Chem. Soc.* 136 (2014) 9236–9239.

[125] K. Vinodgopal, P.V. Kamat, Enhanced rates of photocatalytic degradation of an azo dye using SnO₂/TiO₂ coupled semiconductor thin films, *Environ. Sci. Technol.* 29 (1995) 841–845.

[126] J. Low, J. Yu, M. Jaroniec, S. Wageh, A.A. Al-Ghamdi, Heterojunction photocatalysts, *Adv. Mater.* 29 (2017) 1601694–n/a.

[127] H. Li, W. Tu, Y. Zhou, Z. Zou, Z-scheme photocatalytic systems for promoting photocatalytic performance: recent progress and future challenges, *Adv. Sci.* 3 (2016) 1500389–n/a.

[128] K. Dai, J. Lv, L. Lu, C. Liang, L. Geng, G. Zhu, A facile fabrication of plasmonic g-C₃N₄/Ag₂WO₄/Ag ternary heterojunction visible-light photocatalyst, *Mater. Chem. Phys.* 177 (2016) 529–537.

[129] Y. Liu, J. Kong, J. Yuan, W. Zhao, X. Zhu, C. Sun, J. Xie, Enhanced photocatalytic activity over flower-like sphere Ag/Ag₂CO₃/BiVO₄ plasmonic heterojunction photocatalyst for tetracycline degradation, *Chem. Eng. J.* (2017).

[130] K. Ji, H. Arandiyani, P. Liu, L. Zhang, J. Han, Y. Xue, J. Hou, H. Dai, Interfacial insights into 3D plasmonic multijunction nanoarchitecture toward efficient photocatalytic performance, *Nano Energy* 27 (2016) 515–525.

[131] J. Li, S.K. Cushing, P. Zheng, T. Senty, F. Meng, A.D. Bristow, A. Manivannan, N. Wu, Solar hydrogen generation by a CdS–Au–TiO₂ sandwich nanorod array enhanced with Au nanoparticle as electron relay and plasmonic photosensitizer, *J. Am. Chem. Soc.* 136 (2014) 8438–8449.

[132] J. Li, S.K. Cushing, P. Zheng, F. Meng, D. Chu, N. Wu, Plasmon-induced photonic and energy-transfer enhancement of solar water splitting by a hematite nanorod array, *Nat. Commun.* 4 (2013) 2651.

[133] H. Gao, C. Liu, H.E. Jeong, P. Yang, Plasmon-enhanced photocatalytic activity of iron oxide on gold nanopillars, *ACS Nano* 6 (2012) 234–240.

[134] O. Bunsho, Preparing articles on photocatalysis—beyond the illusions, misconceptions, and speculation, *Chem. Lett.* 37 (2008) 216–229.

[135] Z. Yin, Y. Wang, C. Song, L. Zheng, N. Ma, X. Liu, S. Li, L. Lin, M. Li, Y. Xu, W. Li, G. Hu, Z. Fang, D. Ma, Hybrid Au–Ag nanostructures for enhanced plasmon-driven catalytic selective hydrogenation through visible light irradiation and surface-enhanced Raman scattering, *J. Am. Chem. Soc.* 140 (2018) 864–867.

[136] A. Sousa-Castillo, M. Comesáñ-Hermo, B. Rodríguez-González, M. Pérez-Lorenzo, Z. Wang, X.-T. Kong, A.O. Govorov, M.A. Correa-Duarte, Boosting hot electron-driven photocatalysis through anisotropic plasmonic nanoparticles with hot spots in Au–TiO₂ nanoarchitectures, *J. Phys. Chem. C* 120 (2016) 11690–11699.

[137] Z. Quan, Y. Wang, J. Fang, High-index faceted noble metal nanocrystals, *Acc. Chem. Res.* 46 (2013) 191–202.

[138] Q. Zhang, H. Wang, Facet-dependent catalytic activities of Au nanoparticles enclosed by high-index facets, *ACS Catal.* 4 (2014) 4027–4033.

[139] C. Clavero, Plasmon-induced hot-electron generation at nanoparticle/metal-oxide interfaces for photovoltaic and photocatalytic devices, *Nat. Photon.* 8 (2014) 95–103.

[140] J.I.L. Chen, G. von Freymann, V. Kitaev, G.A. Ozin, Effect of disorder on the optically amplified photocatalytic efficiency of titania inverse opals, *J. Am. Chem. Soc.* 129 (2007) 1196–1202.

[141] J.I.L. Chen, E. Loso, N. Ebrahim, G.A. Ozin, Synergy of slow photon and chemically amplified photochemistry in platinum nanocluster-loaded inverse titania opals, *J. Am. Chem. Soc.* 130 (2008) 5420–5421.

[142] H. Zhao, M. Wu, J. Liu, Z. Deng, Y. Li, B.-L. Su, Synergistic promotion of solar-driven H₂ generation by three-dimensionally ordered macroporous structured TiO₂–Au–CdS ternary photocatalyst, *Appl. Catal. B: Environ.* 184 (2016) 182–190.

[143] Y. Lu, H. Yu, S. Chen, X. Quan, H. Zhao, Integrating plasmonic nanoparticles with TiO₂ photonic crystal for enhancement of visible-light-driven photocatalysis, *Environ. Sci. Technol.* 46 (2012) 1724–1730.

[144] D. Wang, Y. Li, G. Li Puma, C. Wang, P. Wang, W. Zhang, Q. Wang, Ag/AgCl@helical chiral TiO₂ nanofibers as a visible-light driven plasmon photocatalyst, *Chem. Commun.* 49 (2013) 10367–10369.

[145] C.-T. Dinh, H. Yen, F. Kleitz, T.-O. Do, Three-dimensional ordered assembly of thin-shell Au/TiO₂ hollow nanospheres for enhanced visible-light-driven photocatalysis, *Angew. Chem. Int. Ed.* 53 (2014) 6618–6623.

[146] C. Wang, D. Astruc, Nanogold plasmonic photocatalysis for organic synthesis and clean energy conversion, *Chem. Soc. Rev.* 43 (2014) 7188–7216.

[147] Q. Zhang, I. Lee, J. Ge, F. Zaera, Y. Yin, Surface-protected etching of mesoporous oxide shells for the stabilization of metal nanocatalysts, *Adv. Funct. Mater.* 20 (2010) 2201–2214.

[148] Q. Zhang, D.Q. Lima, I. Lee, F. Zaera, M. Chi, Y. Yin, A highly active titanium dioxide based visible-light photocatalyst with nonmetal doping and plasmonic metal decoration, *Angew. Chem. Int. Ed.* 50 (2011) 7088–7092.

[149] Y. Wu, H. Liu, J. Zhang, F. Chen, Enhanced photocatalytic activity of nitrogen-doped titania by deposited with gold, *J. Phys. Chem. C* 113 (2009) 14689–14695.

[150] K. Yu, Y. Tian, T. Tatsuma, Size effects of gold nanoparticles on plasmon-induced photocurrents of gold-TiO₂ nanocomposites, *Phys. Chem. Chem. Phys.* 8 (2006) 5417–5420.

[151] J. Li, S.K. Cushing, J. Bright, F. Meng, T.R. Senty, P. Zheng, A.D. Bristow, N. Wu, Ag@Cu₂O core-shell nanoparticles as visible-light plasmonic photocatalysts, *ACS Catal.* 3 (2013) 47–51.

[152] S.W. Verbruggen, M. Keulemans, M. Filippousi, D. Flahaut, G. Van Tendeloo, S. Lacombe, J.A. Martens, S. Lenaerts, Plasmonic gold–silver alloy on TiO₂ photocatalysts with tunable visible light activity, *Appl. Catal. B: Environ.* 156–157 (2014) 116–121.

[153] P. Wang, B. Huang, X. Qin, X. Zhang, Y. Dai, J. Wei, M.-H. Whangbo, Ag@AgCl: a highly efficient and stable photocatalyst active under visible light, *Angew. Chem. Int. Ed.* 47 (2008) 7931–7933.

[154] Y. Bi, J. Ye, Direct conversion of commercial silver foils into high aspect ratio AgBr nanowires with enhanced photocatalytic properties, *Chemistry* 16 (2010) 10327–10331.

[155] C. Hu, T. Peng, X. Hu, Y. Nie, X. Zhou, J. Qu, H. He, Plasmon-induced photodegradation of toxic pollutants with Ag–AgI/Al₂O₃ under visible-light irradiation, *J. Am. Chem. Soc.* 132 (2010) 857–862.

[156] R. Kant, Textile dyeing industry an environmental hazard, *Nat. Sci.* 04 (01) (2012) 5.

[157] X. Yan, T. Ohno, K. Nishijima, R. Abe, B. Ohtani, Is methylene blue an appropriate substrate for a photocatalytic activity test? A study with visible-light responsive titania, *Chem. Phys. Lett.* 429 (2006) 606–610.

[158] W.-T. Chang, S.-J. Chen, C.-Y. Chang, Y.-H. Liu, C.-H. Chen, C.-H. Yang, L.C.-S. Chou, J.-C. Chang, L.-C. Cheng, W.-S. Kuo, J.-Y. Wang, Effect of size-dependent photodestructive efficacy by gold nanomaterials with multiphoton laser, *ACS Appl. Mater. Interfaces* 7 (2015) 17318–17329.

[159] J.B. Joo, M. Dahl, N. Li, F. Zaera, Y. Yin, Tailored synthesis of mesoporous TiO₂ hollow nanostructures for catalytic applications, *Energy Environ. Sci.* 6 (2013) 2082–2092.

[160] J. Qin, J. Huo, P. Zhang, J. Zeng, T. Wang, H. Zeng, Improving the photocatalytic hydrogen production of Ag/g-C₃N₄ nanocomposites by dye-sensitization under visible light irradiation, *Nanoscale* 8 (2016) 2249–2259.

[161] Y. Qin, R. Che, C. Liang, J. Zhang, Z. Wen, Synthesis of Au and Au–CuO cubic microcages via an in situ sacrificial template approach, *J. Mater. Chem.* 21 (2011) 3960–3965.

[162] D. Chen, S.H. Yoo, Q. Huang, G. Ali, S.O. Cho, Sonochemical synthesis of Ag/AgCl nanocubes and their efficient visible-light-driven photocatalytic performance, *Chemistry* 18 (2012) 5192–5200.

[163] M. Ye, Q. Zhang, Y. Hu, J. Ge, Z. Lu, L. He, Z. Chen, Y. Yin, Magnetically recoverable core–shell nanocomposites with enhanced photocatalytic activity, *Chemistry* 16 (2010) 6243–6250.

[164] H. Zhang, X. Fan, X. Quan, S. Chen, H. Yu, Graphene sheets grafted Ag@AgCl hybrid with enhanced plasmonic photocatalytic activity under visible light, *Environ. Sci. Technol.* 45 (2011) 5731–5736.

[165] X. Li, W. Cai, J. An, S. Kim, J. Nah, D. Yang, R. Piner, A. Velamakanni, I. Jung, E. Tutuc, S.K. Banerjee, L. Colombo, R.S. Ruoff, Large-area synthesis of high-quality and uniform graphene films on copper foils, *Science* 324 (2009) 1312–1314.

[166] K.S. Novoselov, A.K. Geim, S.V. Morozov, D. Jiang, Y. Zhang, S.V. Dubonos, I.V. Grigorieva, A.A. Firsov, Electric field effect in atomically thin carbon films, *Science* 306 (2004) 666–669.

[167] M. Wang, J. Han, H. Xiong, R. Guo, Y. Yin, Nanostructured hybrid shells of r-GO/AuNP/m-TiO₂ as highly active photocatalysts, *ACS Appl. Mater. Interfaces* 7 (2015) 6909–6918.

[168] S. Mosleh, M.R. Rahimi, M. Ghaedi, K. Dashtian, S. Hajati, S. Wang, Ag₃PO₄/AgBr/Ag-HKUST-1-MOF composites as novel blue LED light active photocatalyst for enhanced degradation of ternary mixture of dyes in a rotating packed bed reactor, *Chem. Eng. Process. Process Intensif.* 114 (2017) 24–38.

[169] Y. Zhao, N. Kornienko, Z. Liu, C. Zhu, S. Asahina, T.R. Kuo, W. Bao, C. Xie, A. Hexemer, O. Terasaki, P. Yang, O.M. Yaghi, Mesoscopic constructs of ordered and oriented metal-organic frameworks on plasmonic silver nanocrystals, *J. Am. Chem. Soc.* 137 (2015) 2199–2202.

[170] B. Tian, R. Dong, J. Zhang, S. Bao, F. Yang, J. Zhang, Sandwich-structured AgCl@Ag@TiO₂ with excellent visible-light photocatalytic activity for organic pollutant degradation and *E. coli* K12 inactivation, *Appl. Catal. B: Environ.* 158 (2014) 76–84.

[171] W. Zhao, Y. Guo, S. Wang, H. He, C. Sun, S. Yang, A novel ternary plasmonic photocatalyst: ultrathin g-C₃N₄ nanosheet hybridized by Ag/AgVO₃ nanoribbons with enhanced visible-light photocatalytic performance, *Appl. Catal. B: Environ.* 165 (2015) 335–343.

[172] X. Bai, R. Zong, C. Li, D. Liu, Y. Liu, Y. Zhu, Enhancement of visible photocatalytic activity via Ag@g-C₃N₄ core–shell plasmonic composite, *Appl. Catal. B: Environ.*

147 (2014) 82–91.

[173] J. Yu, G. Dai, B. Huang, Fabrication and characterization of visible-light-driven plasmonic photocatalyst Ag/AgCl/TiO₂ nanotube arrays, *J. Phys. Chem. C* 113 (2009) 16394–16401.

[174] M. Zhu, P. Chen, M. Liu, Graphene oxide enwrapped Ag/AgX (X = Br, Cl) nanocomposite as a highly efficient visible-light plasmonic photocatalyst, *ACS Nano* 5 (2011) 4529–4536.

[175] J. Xiong, Z. Li, J. Chen, S. Zhang, L. Wang, S. Dou, Facile synthesis of highly efficient one-dimensional plasmonic photocatalysts through Ag@Cu₂O Core–Shell heteronanowires, *ACS Appl. Mater. Interfaces* 6 (2014) 15716–15725.

[176] Q. Xiang, J. Yu, B. Cheng, H.C. Ong, Microwave-hydrothermal preparation and visible-light photoactivity of plasmonic photocatalyst Ag-TiO₂ nanocomposite hollow spheres, *Chemistry* 5 (2010) 1466–1474.

[177] H. Zhu, X. Chen, Z. Zheng, X. Ke, E. Jaitinen, J. Zhao, C. Guo, T. Xie, D. Wang, Mechanism of supported gold nanoparticles as photocatalysts under ultraviolet and visible light irradiation, *Chem. Commun.* (2009) 7524–7526.

[178] D. Wang, Y. Li, G. Li Puma, C. Wang, P. Wang, W. Zhang, Q. Wang, Mechanism and experimental study on the photocatalytic performance of Ag/AgCl @ chiral TiO₂ nanofibers photocatalyst: the impact of wastewater components, *J. Hazard. Mater.* 285 (2015) 277–284.

[179] W. He, Y. Liu, W.G. Warner, J.-J. Yin, Electron spin resonance spectroscopy for the study of nanomaterial-mediated generation of reactive oxygen species, *J. Food Drug Anal.* 22 (2014) 49–63.

[180] K.-i. Ishibashi, A. Fujishima, T. Watanabe, K. Hashimoto, Detection of active oxidative species in TiO₂ photocatalysis using the fluorescence technique, *Electrochim. Commun.* 2 (2000) 207–210.

[181] B. Petrie, R. Barden, B. Kasprzyk-Hordern, A review on emerging contaminants in wastewaters and the environment: current knowledge, understudied areas and recommendations for future monitoring, *Water Res.* 72 (2015) 3–27.

[182] D. Wang, Y. Li, G. Li, C. Wang, W. Zhang, Q. Wang, Modeling of quantitative effects of water components on the photocatalytic degradation of 17 α -ethynylestradiol in a modified flat plate serpentine reactor, *J. Hazard. Mater.* 254–255 (2013) 64–71.

[183] Y. Li, Y. Wang, L. Liu, D. Wang, W. Zhang, Ag/ZnO hollow sphere composites: reusable photocatalyst for photocatalytic degradation of 17 α -ethynylestradiol, *Environ. Sci. Pollut. Res.* 21 (2014) 5177–5186.

[184] W. Zhang, Y. Li, C. Wang, P. Wang, Q. Wang, D. Wang, Mechanisms of simultaneous hydrogen production and estrogenic activity removal from secondary effluent though solar photocatalysis, *Water Res.* 47 (2013) 3173–3182.

[185] M. Martins, C. Mourato, S. Sanches, J.P. Noronha, M.T.B. Crespo, I.A.C. Pereira, Biogenic platinum and palladium nanoparticles as new catalysts for the removal of pharmaceutical compounds, *Water Res.* 108 (2017) 160–168.

[186] L. Jiang, G. Zhou, J. Mi, Z. Wu, Fabrication of visible-light-driven one-dimensional anatase TiO₂/Ag heterojunction plasmonic photocatalyst, *Catal. Commun.* 24 (2012) 48–51.

[187] X. Zhang, L. Wang, C. Liu, Y. Ding, S. Zhang, Y. Zeng, Y. Liu, S. Luo, A bamboo-inspired hierarchical nanoarchitecture of Ag/CuO/TiO₂ nanotube array for highly photocatalytic degradation of 2,4-dinitrophenol, *J. Hazard. Mater.* 313 (2016) 244–252.

[188] S.K. Bhunia, N.R. Jana, Reduced graphene oxide–silver nanoparticle composite as visible light photocatalyst for degradation of colorless endocrine disruptors, *ACS Appl. Mater. Interfaces* 6 (2014) 20085–20092.

[189] S. Huang, Y. Xu, Z. Chen, M. Xie, H. Xu, M. He, H. Li, Q. Zhang, A core–shell structured magnetic Ag/AgBr@Fe₂O₃ composite with enhanced photocatalytic activity for organic pollutant degradation and antibacterium, *RSC Adv.* 5 (2015) 71035–71045.

[190] Y. Liu, G. Zhu, J. Gao, M. Hojaberdiel, R. Zhu, X. Wei, Q. Guo, P. Liu, Enhanced photocatalytic activity of Bi₄Ti₃O₁₂ nanosheets by Fe³⁺-doping and the addition of Au nanoparticles: photodegradation of Phenol and bisphenol A, *Appl. Catal. B: Environ.* 200 (2017) 72–82.

[191] H. Dimitrova, V.M. Daskalaki, Z. Frontistis, D.I. Kondarides, P. Panagiotopoulou, N.P. Xekoukoulou, D. Mantzavinos, Solar photocatalysis for the abatement of emerging micro-contaminants in wastewater: synthesis, characterization and testing of various TiO₂ samples, *Appl. Catal. B: Environ.* 117 (2012) 283–291.

[192] J.-C. Sin, S.-M. Lam, A.R. Mohamed, K.-T. Lee, Degrading endocrine disrupting chemicals from wastewater by TiO₂ photocatalysis: a review, *Int. J. Photoenergy* 2012 (2012).

[193] E.J. Rosenfeldt, K.G. Linden, Degradation of endocrine disrupting chemicals bisphenol A, ethinyl estradiol, and estradiol during UV photolysis and advanced oxidation processes, *Environ. Sci. Technol.* 38 (2004) 5476–5483.

[194] H.M. Coleman, E.J. Routledge, J.P. Sumpter, B.R. Egging, J.A. Byrne, Rapid loss of estrogenicity of steroid estrogens by UVA photolysis and photocatalysis over an immobilised titanium dioxide catalyst, *Water Res.* 38 (2004) 3233–3240.

[195] D. Wang, Y. Li, G. Li Puma, P. Lianos, C. Wang, P. Wang, Photoelectrochemical cell for simultaneous electricity generation and heavy metals recovery from wastewater, *J. Hazard. Mater.* 323 (Part B) (2017) 681–689.

[196] D. Wang, Y. Li, G. Li Puma, C. Wang, P. Wang, W. Zhang, Q. Wang, Dye-sensitized photoelectrochemical cell on plasmonic Ag/AgCl @ chiral TiO₂ nanofibers for treatment of urban wastewater effluents, with simultaneous production of hydrogen and electricity, *Appl. Catal. B: Environ.* 168–169 (2015) 25–32.

[197] H. Kyung, J. Lee, W. Choi, Simultaneous and synergistic conversion of dyes and heavy metal ions in aqueous TiO₂ suspensions under visible-light illumination, *Environ. Sci. Technol.* 39 (2005) 2376–2382.

[198] C. Zhou, Z. Wang, A. Ontiveros-Valencia, M. Long, C.-y. Lai, H.-p. Zhao, S. Xia, B.E. Rittmann, Coupling of Pd nanoparticles and denitrifying biofilm promotes H₂-based nitrate removal with greater selectivity towards N₂, *Appl. Catal. B: Environ.* 206 (2017) 461–470.

[199] D. Yue, X. Qian, Y. Zhao, Photocatalytic remediation of ionic pollutant, *Sci. Bull.* 60 (2015) 1791–1806.

[200] J.B. Umland, J.M. Bellama, *General Chemistry*, 2nd ed., West Publishing, St. Paul, Minnesota, 1996.

[201] D. Chen, A.K. Ray, Removal of toxic metal ions from wastewater by semiconductor photocatalysis, *Chem. Eng. Sci.* 56 (2001) 1561–1570.

[202] J. Su, Y. Zhang, S. Xu, S. Wang, H. Ding, S. Pan, G. Wang, G. Li, H. Zhao, Highly efficient and recyclable triple-shelled Ag@Fe₃O₄@SiO₂@TiO₂ photocatalysts for degradation of organic pollutants and reduction of hexavalent chromium ions, *Nanoscale* 6 (2014) 5181–5192.

[203] J.J. Testa, M.A. Grela, M.I. Litter, Heterogeneous photocatalytic reduction of chromium(VI) over TiO₂ particles in the presence of oxalate: involvement of Cr(V) species, *Environ. Sci. Technol.* 38 (2004) 1589–1594.

[204] N. Wang, L. Zhu, K. Deng, Y. She, Y. Yu, H. Tang, Visible light photocatalytic reduction of Cr(VI) on TiO₂ in situ modified with small molecular weight organic acids, *Appl. Catal. B: Environ.* 95 (2010) 400–407.

[205] F.-Q. Shao, J.-J. Feng, X.-X. Lin, L.-Y. Jiang, A.-J. Wang, Simple fabrication of AuPd@Pd core–shell nanocrystals for effective catalytic reduction of hexavalent chromium, *Appl. Catal. B: Environ.* 208 (2017) 128–134.

[206] S. Luo, Y. Xiao, L. Yang, C. Liu, F. Su, Y. Li, Q. Cai, G. Zeng, Simultaneous detoxification of hexavalent chromium and acid orange 7 by a novel Au/TiO₂ heterojunction composite nanotube arrays, *Sep. Purif. Technol.* 79 (2011) 85–91.

[207] Y. Choi, M.S. Koo, A.D. Bokare, D.-h. Kim, D.W. Bahnemann, W. Choi, Sequential process combination of photocatalytic oxidation and dark reduction for the removal of organic pollutants and Cr(VI) using Ag/TiO₂, *Environ. Sci. Technol.* 51 (2017) 3973–3981.

[208] W.J. Youngblood, S.-H.A. Lee, Y. Kobayashi, E.A. Hernandez-Pagan, P.G. Hoertz, T.A. Moore, A.L. Moore, D. Gust, T.E. Mallouk, Photoassisted overall water splitting in a visible light-absorbing dye-sensitized photoelectrochemical cell, *J. Am. Chem. Soc.* 131 (2009) 926–927.

[209] X. Liu, X. Cui, Y. Liu, Y. Yin, Stabilization of ultrafine metal nanocatalysts on thin carbon sheets, *Nanoscale* 7 (2015) 18320–18326.

[210] P.D. Cozzoli, R. Comparelli, E. Fanizza, M.L. Curri, A. Agostiano, D. Laub, Photocatalytic synthesis of silver nanoparticles stabilized by TiO₂ nanorods: a semiconductor/metal nanocomposite in homogeneous nonpolar solution, *J. Am. Chem. Soc.* 126 (2004) 3868–3879.

[211] H.O.N. Tugaen, S. Garcia-Segura, K. Hristovski, P. Westerhoff, Challenges in photocatalytic reduction of nitrate as a water treatment technology, *Sci. Total Environ.* 599 (2017) 1524–1551.

[212] V.M. Daskalaki, M. Antoniadou, G. Li Puma, D.I. Kondarides, P. Lianos, Solar light-responsive Pt/CdS/TiO₂ photocatalysts for hydrogen production and simultaneous degradation of inorganic or organic sacrificial agents in wastewater, *Environ. Sci. Technol.* 44 (2010) 7200–7205.

[213] S.C. Warren, E. Thimmen, Plasmonic solar water splitting, *Energy Environ. Sci.* 5 (2012) 5133–5146.

[214] P. Lianos, Review of recent trends in photoelectrocatalytic conversion of solar energy to electricity and hydrogen, *Appl. Catal. B: Environ.* 210 (2017) 235–254.

[215] T. Luo, J. Bai, J. Li, Q. Zeng, Y. Ji, L. Qiao, X. Li, B. Zhou, Self-driven photoelectrochemical splitting of H₂S for S and H₂ recovery and simultaneous electricity generation, *Environ. Sci. Technol.* 51 (2017) 12965–12971.

[216] Y. Ji, J. Bai, J. Li, T. Luo, L. Qiao, Q. Zeng, B. Zhou, Highly selective transformation of ammonia nitrogen to N₂ based on a novel solar-driven photoelectrocatalytic-chlorine radical reactions system, *Water Res.* 125 (2017) 512–519.

[217] L. Zhu, D.J. Jacob, F.N. Keutsch, L.J. Mickley, R. Scheffe, M. Strum, G. González Abad, K. Chance, K. Yang, B. Rappenglück, D.B. Millet, M. Baasandorj, L. Jaeglé, V. Shah, Formaldehyde (HCHO) as a hazardous air pollutant: mapping surface air concentrations from satellite and inferring cancer risks in the United States, *Environ. Sci. Technol.* (2017).

[218] U.S. Environmental Protection Agency (EPA), U.S. Consumer Product Safety Commission (CPSC), *The Inside Story: A Guide to Indoor Air Quality*, Office of Radiation and Indoor Air (6604J), 1995.

[219] U.S. Consumer Product Safety Commission, *An Update on Formaldehyde*, Bethesda, MD, (2016).

[220] IARC Classifies Formaldehyde as Carcinogenic to Humans, International Agency for Research on Cancer, Lyon, France, 2004 pp. 153.

[221] T. Okachi, M. Onaka, Formaldehyde encapsulated in zeolite: a long-lived, highly activated one-carbon electrophile to carbonyl-ene reactions, *J. Am. Chem. Soc.* 126 (2004) 2306–2307.

[222] W.B. Li, J.X. Wang, H. Gong, Catalytic combustion of VOCs on non-noble metal catalysts, *Catal. Today* 148 (2009) 81–87.

[223] Y. Huang, S. Ho, Y. Lu, R. Niu, L. Xu, J. Cao, S. Lee, Removal of indoor volatile organic compounds via photocatalytic oxidation: a short review and Prospect, *Molecules* 21 (2016) 56.

[224] T. Noguchi, A. Fujishima, P. Sawunyama, K. Hashimoto, Photocatalytic degradation of gaseous formaldehyde using TiO₂ film, *Environ. Sci. Technol.* 32 (1998) 3831–3833.

[225] C. Zhang, H. He, K.-i. Tanaka, Perfect catalytic oxidation of formaldehyde over a

Pt/TiO₂ catalyst at room temperature, *Catal. Commun.* 6 (2005) 211–214.

[226] L. Nie, J. Yu, M. Jaroniec, F.F. Tao, Room-temperature catalytic oxidation of formaldehyde on catalysts, *Catal. Sci. Technol.* 6 (2016) 3649–3669.

[227] H. Tan, J. Wang, S. Yu, K. Zhou, Support morphology-dependent catalytic activity of Pd/CeO₂ for formaldehyde oxidation, *Environ. Sci. Technol.* 49 (2015) 8675–8682.

[228] S. Zhao, Z. Qu, N. Yan, Z. Li, W. Zhu, J. pan, J. Xu, M. Li, Ag-modified AgI-TiO₂ as an excellent and durable catalyst for catalytic oxidation of elemental mercury, *RSC Adv.* 5 (2015) 30841–30850.

[229] Y. Zhang, Z.-R. Tang, X. Fu, Y.-J. Xu, Nanocomposite of Ag–AgBr–TiO₂ as a photoactive and durable catalyst for degradation of volatile organic compounds in the gas phase, *Appl. Catal. B: Environ.* 106 (2011) 445–452.

[230] R. Kaur, B. Pal, Plasmonic coinage metal-TiO₂ hybrid nanocatalysts for highly efficient photocatalytic oxidation under sunlight irradiation, *New J. Chem.* 39 (2015) 5966–5976.

[231] S. Sun, J. Ding, J. Bao, C. Gao, Z. Qi, X. Yang, B. He, C. Li, Photocatalytic degradation of gaseous toluene on Fe-TiO₂ under visible light irradiation: a study on the structure, activity and deactivation mechanism, *Appl. Surf. Sci.* 258 (2012) 5031–5037.

[232] O. Fontelles-Carceller, M.J. Muñoz-Batista, M. Fernández-García, A. Kubacka, Interface effects in sunlight-driven Ag/g-C₃N₄ composite catalysts: study of the toluene photodegradation quantum efficiency, *ACS Appl. Mater. Interfaces* 8 (2016) 2617–2627.

[233] S. Royer, D. Duprez, Catalytic oxidation of carbon monoxide over transition metal oxides, *ChemCatChem* 3 (2011) 24–65.

[234] A.S. Kireev, V.M. Mukhin, S.G. Kireev, V.N. Klushin, S.N. Tkachenko, Preparation and properties of modified hopcalite, *Russ. J. Appl. Chem.* 82 (2009) 169–171.

[235] A. Manasilp, E. Gulari, Selective CO oxidation over Pt/alumina catalysts for fuel cell applications, *Appl. Catal. B: Environ.* 37 (2002) 17–25.

[236] H. Einaga, M. Harada, S. Futamura, T. Ibusuki, Generation of active sites for CO photooxidation on TiO₂ by platinum deposition, *J. Phys. Chem. B* 107 (2003) 9290–9297.

[237] H. Shen, I.-R. Ie, C.-S. Yuan, C.-H. Hung, W.-H. Chen, J. Luo, Y.-H. Jen, Enhanced photocatalytic oxidation of gaseous elemental mercury by TiO₂ in a high temperature environment, *J. Hazard. Mater.* 289 (2015) 235–243.

[238] G.C. Bond, D.T. Thompson, Catalysis by gold, *Catal. Rev. 41* (1999) 319–388.

[239] S. Carrettin, P. Concepción, A. Corma, J.M. López Nieto, V.F. Puntes, Nanocrystalline CeO₂ increases the activity of Au for CO oxidation by two orders of magnitude, *Angew. Chem. Int. Ed.* 43 (2004) 2538–2540.

[240] W.H. Hung, M. Aykol, D. Valley, W. Hou, S.B. Cronin, Plasmon resonant enhancement of carbon monoxide catalysis, *Nano Lett.* 10 (2010) 1314–1318.

[241] Q. Yao, C. Wang, H. Wang, H. Yan, J. Lu, Revisiting the Au particle size effect on TiO₂-coated Au/TiO₂ catalysts in CO oxidation reaction, *J. Phys. Chem. C* 120 (2016) 9174–9183.

[242] K. Skalska, J.S. Miller, S. Ledakowicz, Trends in NO_x abatement: a review, *Sci. Total Environ.* 408 (2010) 3976–3989.

[243] J. Lasek, Y.-H. Yu, J.C.S. Wu, Removal of NO_x by photocatalytic processes, *J. Photochem. Photobiol. C: Photochem. Rev.* 14 (2013) 29–52.

[244] Q. Zhang, Y. Huang, L. Xu, J.-J. Cao, W. Ho, S.C. Lee, Visible-light-active plasmonic Ag–SrTiO₃ nanocomposites for the degradation of NO in air with high selectivity, *ACS Appl. Mater. Interfaces* 8 (2016) 4165–4174.

[245] Y. Duan, M. Zhang, L. Wang, F. Wang, L. Yang, X. Li, C. Wang, Plasmonic Ag-TiO_{2-x} nanocomposites for the photocatalytic removal of NO under visible light with high selectivity: the role of oxygen vacancies, *Appl. Catal. B: Environ.* 204 (2017) 67–77.

[246] C. Su, X. Ran, J. Hu, C. Shao, Photocatalytic process of simultaneous desulfurization and denitrification of flue gas by TiO₂-polyacrylonitrile nanofibers, *Environ. Sci. Technol.* 47 (2013) 11562–11568.

[247] F. Rezaei, A.A. Rownagh, S. Monjezi, R.P. Lively, C.W. Jones, SO_x/NO_x removal from flue gas streams by solid adsorbents: a review of current challenges and future directions, *Energy Fuel* 29 (2015) 5467–5486.

[248] A. Zhang, L. Zhang, H. Lu, G. Chen, Z. Liu, J. Xiang, L. Sun, Facile synthesis of ternary Ag/AgBr-Ag₂CO₃ hybrids with enhanced photocatalytic removal of elemental mercury driven by visible light, *J. Hazard. Mater.* 314 (2016) 78–87.

[249] C.R. McLaren, E.J. Granite, H.W. Pennline, The PCO process for photochemical removal of mercury from flue gas, *Fuel Process. Technol.* 87 (2005) 85–89.

[250] A. Zhang, L. Zhang, X. Chen, Q. Zhu, Z. Liu, J. Xiang, Photocatalytic oxidation removal of HgO using ternary Ag/AgI-Ag₂CO₃ hybrids in wet scrubbing process under fluorescent light, *Appl. Surf. Sci.* 392 (2017) 1107–1116.

[251] Y. Liu, Y.G. Adewuya, A review on removal of elemental mercury from flue gas using advanced oxidation process: chemistry and process, *Chem. Eng. Res. Des.* 112 (2016) 199–250.

[252] Y. Zhou, Y. Kong, S. Kundu, J.D. Cirillo, H. Liang, Antibacterial activities of gold and silver nanoparticles against *Escherichia coli* and *bacillus calmette-guérin*, *J. Nanobiotechnol.* 10 (2012) 19.

[253] Q. Li, S. Mahendra, D.Y. Lyon, L. Brunet, M.V. Liga, D. Li, P.J.J. Alvarez, Antimicrobial nanomaterials for water disinfection and microbial control: potential applications and implications, *Water Res.* 42 (2008) 4591–4602.

[254] M.W. Davidson, Bacteria Cell Structure, (2015).

[255] P. Ganguly, C. Byrne, A. Breen, S.C. Pillai, Antimicrobial activity of photocatalysts: fundamentals, mechanisms, kinetics and recent advances, *Appl. Catal. B: Environ.* 225 (2018) 51–75.

[256] O.K. Dalrymple, E. Stefanakos, M.A. Trotz, D.Y. Goswami, A review of the mechanisms and modeling of photocatalytic disinfection, *Appl. Catal. B: Environ.* 98 (2010) 27–38.

[257] M.J. Hajipour, K.M. Fromm, A. Akbar Ashkarraan, D. Jimenez de Aberasturi, I.R.D. Larramendi, T. Rojo, V. Serpooshan, W.J. Parak, M. Mahmoudi, Antibacterial properties of nanoparticles, *Trends Biotechnol.* 30 (2012) 499–511.

[258] Q.L. Feng, J. Wu, G.Q. Chen, F.Z. Cui, T.N. Kim, J.O. Kim, A mechanistic study of the antibacterial effect of silver ions on *Escherichia coli* and *Staphylococcus aureus*, *J. Biomed. Mater. Res.* 52 (2000) 662–668.

[259] M. Sökmen, F. Candan, Z. Sümer, Disinfection of *E. coli* by the Ag-TiO₂/UV system: lipidperoxidation, *J. Photochem. Photobiol. A Chem.* 143 (2001) 241–244.

[260] I. Sondi, B. Salopek-Sondi, Silver nanoparticles as antimicrobial agent: a case study on *E. coli* as a model for gram-negative bacteria, *J. Colloid Interface Sci.* 275 (2004) 177–182.

[261] Y. Matsumura, K. Yoshikata, S.-i. Kunisaki, T. Tsuchido, Mode of bactericidal action of silver zeolite and its comparison with that of silver nitrate, *Appl. Environ. Microbiol.* 69 (2003) 4278–4281.

[262] J.S. Kim, E. Kuk, K.N. Yu, J.-H. Kim, S.J. Park, H.J. Lee, S.H. Kim, Y.K. Park, Y.H. Park, C.-Y. Hwang, Y.-K. Kim, Y.-S. Lee, D.H. Jeong, M.-H. Cho, Antimicrobial effects of silver nanoparticles, *Nanomed. Nanotechnol. Biol. Med.* 3 (2007) 95–101.

[263] M. Guzman, J. Dille, S. Godet, Synthesis and antibacterial activity of silver nanoparticles against gram-positive and gram-negative bacteria, *Nanomed. Nanotechnol. Biol. Med.* 8 (2012) 37–45.

[264] O. Choi, K.K. Deng, N.-J. Kim, L. Ross, R.Y. Surampalli, Z. Hu, The inhibitory effects of silver nanoparticles, silver ions, and silver chloride colloids on microbial growth, *Water Res.* 42 (2008) 3066–3074.

[265] O.K. Dalrymple, E. Stefanakos, M.A. Trotz, D.Y. Goswami, A review of the mechanisms and modeling of photocatalytic disinfection, *Appl. Catal. B: Environ.* 98 (2010) 27–38.

[266] W. Wang, G. Huang, J.C. Yu, P.K. Wong, Advances in photocatalytic disinfection of bacteria: development of photocatalysts and mechanisms, *J. Environ. Sci.* 34 (2015) 232–247.

[267] N.S. Leyland, J. Podporska-Carroll, J. Browne, S.J. Hinder, B. Quilty, S.C. Pillai, Highly efficient F, Cu doped TiO₂ anti-bacterial visible light active photocatalytic coatings to combat hospital-acquired infections, *Sci. Rep.* 6 (2016) 24770.

[268] K.E. Ebogbodin, C.A. Biggs, Characterization of the extracellular polymeric substances produced by *Escherichia coli* using infrared spectroscopic, proteomic, and aggregation studies, *Biomacromolecules* 9 (2008) 686–695.

[269] Y. Liu, J. Li, X. Qiu, C. Burda, Bactericidal activity of nitrogen-doped metal oxide nanocatalysts and the influence of bacterial extracellular polymeric substances (EPS), *J. Photochem. Photobiol. A Chem.* 190 (2007) 94–100.

[270] A.S. Gong, C.A. Lanzl, D.M. Cwiertny, S.L. Walker, Lack of influence of extracellular polymeric substances (EPS) level on hydroxyl radical mediated disinfection of *Escherichia coli*, *Environ. Sci. Technol.* 46 (2012) 241–249.

[271] G. Huang, D. Xia, T. An, T.W. Ng, H.Y. Yip, G. Li, H. Zhao, P.K. Wong, Dual roles of capsular extracellular polymeric substances in photocatalytic inactivation of *Escherichia coli*: comparison of *E. coli* BW25113 and isogenic mutants, *Appl. Environ. Microbiol.* 81 (2015) 5174–5183.

[272] J. Kiwi, V. Nadtochenko, Evidence for the mechanism of photocatalytic degradation of the bacterial wall membrane at the TiO₂ interface by ATR-FTIR and laser kinetic spectroscopy, *Langmuir* 21 (2005) 4631–4641.

[273] S. Thabet, F. Simonet, M. Lemaire, C. Guillard, P. Cotton, Impact of photocatalysis on fungal cells: depiction of cellular and molecular effects on *Saccharomyces cerevisiae*, *Appl. Environ. Microbiol.* 80 (2014) 7527–7535.

[274] T.Y. Leung, C.Y. Chan, C. Hu, J.C. Yu, P.K. Wong, Photocatalytic disinfection of marine bacteria using fluorescent light, *Water Res.* 42 (2008) 4827–4837.

[275] S. Thabet, M. Weiss-Gayet, F. Dappozze, P. Cotton, C. Guillard, Photocatalysis on yeast cells: toward targets and mechanisms, *Appl. Catal. B: Environ.* 140 (2013) 169–178.

[276] G. Gogniat, S. Dukan, TiO₂ photocatalysis causes DNA damage via fenton reaction-generated hydroxyl radicals during the recovery period, *Appl. Environ. Microbiol.* 73 (2007) 7740–7743.

[277] D. Xia, Z. Shen, G. Huang, W. Wang, J.C. Yu, P.K. Wong, Red phosphorus: an earth-abundant elemental photocatalyst for “Green” bacterial Inactivation under visible light, *Environ. Sci. Technol.* 49 (2015) 6264–6273.

[278] X. Huang, M.A. El-Sayed, Plasmonic photo-thermal therapy (PPTT), *Alexandria J. Med.* 47 (2011) 1–9.

[279] K. Boris, Z. Vladimir, M. Andrei, T. Valery, K. Nikolai, Optical amplification of photothermal therapy with gold nanoparticles and nanoclusters, *Nanotechnology* 17 (2006) 5167.

[280] V.P. Zharov, K.E. Mercer, E.N. Galitovskaya, M.S. Smeltzer, Photothermal nanotherapy and nanodiagnosis for selective killing of bacteria targeted with gold nanoparticles, *Biophys. J.* 90 (2006) 619–627.

[281] R.S. Norman, J.W. Stone, A. Gole, C.J. Murphy, T.L. Sabo-Attwood, Targeted photothermal lysis of the pathogenic bacteria, *Pseudomonas aeruginosa*, with gold nanorods, *Nano Lett.* 8 (2008) 302–306.

[282] W. Xu, M. Wang, Z. Li, X. Wang, Y. Wang, M. Xing, Y. Yin, Chemical transformation of colloidal nanostructures with morphological preservation by surface-protection with capping ligands, *Nano Lett.* 17 (2017) 2713–2718.

[283] J.-S. Lee, M.S. Han, C.A. Mirkin, Colorimetric detection of mercuric ion (Hg²⁺) in

aqueous media using DNA-functionalized gold nanoparticles, *Angew. Chem. Int. Ed.* 46 (2007) 4093–4096.

[284] Y. Zhou, S. Wang, K. Zhang, X. Jiang, Visual detection of Copper(II) by azide- and alkyne-functionalized gold nanoparticles using click chemistry, *Angew. Chem. Int. Ed.* 47 (2008) 7454–7456.

[285] J. Du, L. Jiang, Q. Shao, X. Liu, R.S. Marks, J. Ma, X. Chen, Colorimetric detection of mercury ions based on plasmonic nanoparticles, *Small* 9 (2013) 1467–1481.

[286] S.A. Khan, A.K. Singh, D. Senapati, Z. Fan, P.C. Ray, Bio-conjugated popcorn shaped gold nanoparticles for targeted photothermal killing of multiple drug resistant *Salmonella* DT104, *J. Mater. Chem.* 21 (2011) 17705–17709.

[287] C. Liu, X. Xie, W. Zhao, N. Liu, P.A. Maraccini, L.M. Sasseboure, A.B. Boehm, Y. Cui, Conducting nanospunge electroporation for affordable and high-efficiency disinfection of bacteria and viruses in water, *Nano Lett.* 13 (2013) 4288–4293.

[288] D.T. Schoen, A.P. Schoen, L. Hu, H.S. Kim, S.C. Heilshorn, Y. Cui, High speed water sterilization using one-dimensional nanostructures, *Nano Lett.* 10 (2010) 3628–3632.

[289] M. Yao, G. Mainelis, H.R. An, Inactivation of microorganisms using electrostatic fields, *Environ. Sci. Technol.* 39 (2005) 3338–3344.

[290] Z.-Y. Huo, X. Xie, T. Yu, Y. Lu, C. Feng, H.-Y. Hu, Nanowire-modified three-dimensional electrode enabling low-voltage electroporation for water disinfection, *Environ. Sci. Technol.* 50 (2016) 7641–7649.

[291] T. Kotnik, W. Frey, M. Sack, S. Haberl Meglič, M. Peterka, D. Miklavčič, Electroporation-based applications in biotechnology, *Trends Biotechnol.* 33 (2015) 480–488.

[292] D. Wang, B. Zhu, X. He, Z. Zhu, G. Hutchins, P. Xu, W.-N. Wang, Iron oxide nanowire-based filter for inactivation of airborne bacteria, *Environ. Sci. Nano* (2018).

[293] S. Dervin, J. Murphy, R. Aviles, S.C. Pillai, M. Garvey, An in vitro cytotoxicity assessment of graphene nanosheets on alveolar cells, *Appl. Surf. Sci.* 434 (2018) 1274–1284.

[294] S.J. Klaine, P.J.J. Alvarez, G.E. Batley, T.F. Fernandes, R.D. Handy, D.Y. Lyon, S. Mahendra, M.J. McLaughlin, J.R. Lead, Nanomaterials in the environment: behavior, fate, bioavailability, and effects, *Environ. Toxicol. Chem.* 27 (2008) 1825–1851.

[295] V.L. Colvin, The potential environmental impact of engineered nanomaterials, *Nat. Biotechnol.* 21 (2003) 1166.

[296] M.R. Wiesner, G.V. Lowry, P. Alvarez, D. Dionysiou, P. Biswas, Assessing the risks of manufactured nanomaterials, *Environ. Sci. Technol.* 40 (2006) 4336–4345.

[297] J. Fabrega, S.N. Luoma, C.R. Tyler, T.S. Galloway, J.R. Lead, Silver nanoparticles: behaviour and effects in the aquatic environment, *Environ. Int.* 37 (2011) 517–531.

[298] S.A. Blaser, M. Scheringer, M. MacLeod, K. Hungerbühler, Estimation of cumulative aquatic exposure and risk due to silver: contribution of nano-functionalized plastics and textiles, *Sci. Total Environ.* 390 (2008) 396–409.

[299] A. Caballero-Guzman, B. Nowack, A critical review of engineered nanomaterial release data: are current data useful for material flow modeling? *Environ. Pollut.* 213 (2016) 502–517.

[300] A. Azimzada, N. Tufenkji, K.J. Wilkinson, Transformations of silver nanoparticles in wastewater effluents: links to Ag bioavailability, *Environ. Sci. Nano* 4 (2017) 1339–1349.

[301] J.L. Gardea-Torresdey, C.M. Rico, J.C. White, Trophic transfer, transformation, and impact of engineered nanomaterials in terrestrial environments, *Environ. Sci. Technol.* 48 (2014) 2526–2540.

[302] G.E. Batley, J.K. Kirby, M.J. McLaughlin, Fate and risks of nanomaterials in aquatic and terrestrial environments, *Acc. Chem. Res.* 46 (2013) 854–862.

[303] D. Lin, X. Tian, F. Wu, B. Xing, Fate and transport of engineered nanomaterials in the environment, *J. Environ. Qual.* 39 (2010) 1896–1908.

[304] J. Olabarrieta, S. Zorita, I. Peña, N. Rioja, O. Monzón, P. Benguria, L. Scifo, Aging of photocatalytic coatings under a water flow: long run performance and TiO₂ nanoparticles release, *Appl. Catal. B: Environ.* 123–124 (2012) 182–192.

[305] G.V. Lowry, B.P. Espinasse, A.R. Badireddy, C.J. Richardson, B.C. Reinsch, L.D. Bryant, A.J. Bone, A. Deonarine, S. Chae, M. Therezien, B.P. Colman, H. Hsu-Kim, E.S. Bernhardt, C.W. Matson, M.R. Wiesner, Long-term transformation and fate of manufactured Ag nanoparticles in a simulated large scale freshwater emergent wetland, *Environ. Sci. Technol.* 46 (2012) 7027–7036.

[306] K.L. Garner, A.A. Keller, Emerging patterns for engineered nanomaterials in the environment: a review of fate and toxicity studies, *J. Nanopart. Res.* 16 (2014) 2503.

[307] Y. Sun, Y. Xia, Shape-controlled synthesis of gold and silver nanoparticles, *Science* 298 (2002) 2176–2179.

[308] Y. Yin, A.P. Alivisatos, Colloidal nanocrystal synthesis and the organic-inorganic interface, *Nature* 437 (2005) 664–670.

[309] W.M. Moore, P.J. Codella, Oxidation of silver films by atomic oxygen, *J. Phys. Chem.* 92 (1988) 4421–4426.

[310] M.M. Shahjamali, Y. Zhou, N. Zaraee, C. Xue, J. Wu, N. Large, C.M. McGuirk, F. Boey, V. Dravid, Z. Cui, G.C. Schatz, C.A. Mirkin, Ag–Ag₂S hybrid nanoparticles: structural versus plasmonic evolution, *ACS Nano* 10 (2016) 5362–5373.

[311] J. Zeng, M. Li, A. Liu, F. Feng, T. Zeng, W. Duan, M. Li, M. Gong, C.Y. Wen, Y. Yin, Au/AgI dimeric nanoparticles for highly selective and sensitive colorimetric detection of hydrogen sulfide, *Adv. Funct. Mater.* (2018) 1800515.

[312] C. Levard, E.M. Hotze, G.V. Lowry, G.E. Brown, Environmental transformations of silver nanoparticles: impact on stability and toxicity, *Environ. Sci. Technol.* 46 (2012) 6900–6914.

[313] C. Liu, W. Leng, P.J. Vikesland, Controlled evaluation of the impacts of surface coatings on silver nanoparticle dissolution rates, *Environ. Sci. Technol.* 52 (2018) 2726–2734.

[314] M. Levak, P. Burić, M. Dutour Sikirić, D. Domazet Jurašin, N. Mikac, N. Bačić, R. Drexel, F. Meier, Ž. Jakšić, D.M. Lyons, Effect of protein corona on silver nanoparticle stabilization and ion release kinetics in artificial seawater, *Environ. Sci. Technol.* 51 (2017) 1259–1266.

[315] M.S. McKee, J. Filszer, Impacts of metal-based engineered nanomaterials on soil communities, *Environ. Sci. Nano* 3 (2016) 506–533.

[316] D. Lu, Q. Liu, T. Zhang, Y. Cai, Y. Yin, G. Jiang, Stable silver isotope fractionation in the natural transformation process of silver nanoparticles, *Nat. Nanotechnol.* 11 (2016) 682.

[317] X. Yang, C. Jiang, H. Hsu-Kim, A.R. Badireddy, M. Dykstra, M. Wiesner, D.E. Hinton, J.N. Meyer, Silver nanoparticle behavior, uptake, and toxicity in *Caenorhabditis elegans*: effects of natural organic matter, *Environ. Sci. Technol.* 48 (2014) 3486–3495.

[318] Y. Jung, G. Metreveli, C.-B. Park, S. Baik, G.E. Schaumann, Implications of Pony Lake fulvic acid for the aggregation and dissolution of oppositely charged surface-coated silver nanoparticles and their ecotoxicological effects on *Daphnia magna*, *Environ. Sci. Technol.* 52 (2018) 436–445.

[319] X. Yang, S. Lin, M.R. Wiesner, Influence of natural organic matter on transport and retention of polymer coated silver nanoparticles in porous media, *J. Hazard. Mater.* 264 (2014) 161–168.

[320] N.K. Geitner, S.M. Marinakos, C. Guo, N. O'Brien, M.R. Wiesner, Nanoparticle surface affinity as a predictor of trophic transfer, *Environ. Sci. Technol.* 50 (2016) 6663–6669.

[321] A.M. Alkilany, S.E. Lohse, C.J. Murphy, The gold standard: gold nanoparticle libraries to understand the nano-bio interface, *Acc. Chem. Res.* 46 (2013) 650–661.

[322] J.L. Ferry, P. Craig, C. Hexel, P. Sisco, R. Frey, P.L. Pennington, M.H. Fulton, I.G. Scott, A.W. Decho, S. Kashiwada, C.J. Murphy, T.J. Shaw, Transfer of gold nanoparticles from the water column to the estuarine food web, *Nat. Nanotechnol.* 4 (2009) 441.

[323] I.N. Throback, M. Johansson, M. Rosenquist, M. Pell, M. Hansson, S. Hallin, Silver (Ag⁺) reduces denitrification and induces enrichment of novel nirK genotypes in soil, *FEMS Microbiol. Lett.* 270 (2007) 189–194.

[324] J.W. Metch, N.D. Burrows, C.J. Murphy, A. Pruden, P.J. Vikesland, Metagenomic analysis of microbial communities yields insight into impacts of nanoparticle design, *Nat. Nanotechnol.* 13 (2018) 253–259.

[325] J.D. Moore, J.P. Stegemeier, K. Bibby, S.M. Marinakos, G.V. Lowry, K.B. Gregory, Impacts of pristine and transformed Ag and Cu engineered nanomaterials on surficial sediment microbial communities appear short-lived, *Environ. Sci. Technol.* 50 (2016) 2641–2651.

[326] J.M. Unrine, S.E. Hunyadi, O.V. Tsyusko, W. Rao, W.A. Shoultz-Wilson, P.M. Bertsch, Evidence for bioavailability of Au nanoparticles from soil and bio-distribution within earthworms (*Eisenia fetida*), *Environ. Sci. Technol.* 44 (2010) 8308–8313.

[327] A. Baun, N.B. Hartmann, K. Grieger, K.O. Kusk, Ecotoxicity of engineered nanoparticles to aquatic invertebrates: a brief review and recommendations for future toxicity testing, *Ecotoxicology* 17 (2008) 387–395.

[328] N. Zuverza-Mena, D. Martínez-Fernández, W. Du, J.A. Hernandez-Viecas, N. Bonilla-Bird, M.L. López-Moreno, M. Komárek, J.R. Peralta-Videa, J.L. Gardea-Torresdey, Exposure of engineered nanomaterials to plants: insights into the physiological and biochemical responses—a review, *Plant Physiol. Biochem.* 110 (2017) 236–264.

[329] L. Yuan, C.J. Richardson, M. Ho, C.W. Willis, B.P. Colman, M.R. Wiesner, Stress responses of aquatic plants to silver nanoparticles, *Environ. Sci. Technol.* 52 (2018) 2558–2565.

[330] J.P. Stegemeier, B.P. Colman, F. Schwab, M.R. Wiesner, G.V. Lowry, Uptake and distribution of silver in the aquatic plant *Landoltia punctata* (Duckweed) exposed to silver and silver sulfide nanoparticles, *Environ. Sci. Technol.* 51 (2017) 4936–4943.

[331] A. Avellan, F. Schwab, A. Masion, P. Chaurand, D. Borschneck, V. Vidal, J. Rose, C. Santaella, C. Levard, Nanoparticle uptake in plants: gold nanoparticle localized in roots of *Arabidopsis thaliana* by X-ray computed nanotomography and hyperspectral imaging, *Environ. Sci. Technol.* 51 (2017) 8682–8691.

[332] Y.-S. Chen, Y.-C. Hung, I. Liau, G.S. Huang, Assessment of the in vivo toxicity of gold nanoparticles, *Nanoscale Res. Lett.* 4 (2009) 858.

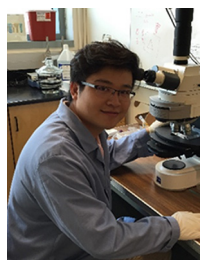
[333] M.A. Maurer-Jones, I.L. Gunsolus, C.J. Murphy, C.L. Haynes, Toxicity of engineered nanoparticles in the environment, *Anal. Chem.* 85 (2013) 3036–3049.

[334] A.M. Alkilany, C.J. Murphy, Toxicity and cellular uptake of gold nanoparticles: what we have learned so far? *J. Nanopart. Res.* 12 (2010) 2313–2333.

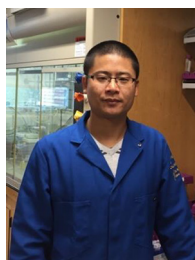
[335] N. Khlebtsov, L. Dykman, Biodistribution and toxicity of engineered gold nanoparticles: a review of in vitro and in vivo studies, *Chem. Soc. Rev.* 40 (2011) 1647–1671.

[336] M.P. Tsang, E. Kikuchi-Uehara, G.W. Sonnemann, C. Aymonier, M. Hirao, Evaluating nanotechnology opportunities and risks through integration of life-cycle and risk assessment, *Nat. Nanotechnol.* 12 (2017) 734.

[337] C. Beer, R. Foldbjerg, Y. Hayashi, D.S. Sutherland, H. Autrup, Toxicity of silver nanoparticles—nanoparticle or silver ion? *Toxicol. Lett.* 208 (2012) 286–292.



Dawei Wang received his B.E. and Ph.D. degrees in environmental engineering from Hohai University, China in 2011 and 2016, respectively. During 2014–2016, he also worked as a visiting student in the Department of Chemistry at University of California, Riverside, USA. Currently, he is a postdoc research fellow at Virginia Commonwealth University, USA. His research mainly focuses on the development of novel materials/processes for water treatment. He was the recipient of National Scholarship (2012, 2013, and 2015) from the Ministry of Education, China and the recipient of Outstanding Award of the Baogang Education Scholarship 2015.



Jingbin Zeng obtained his PhD degree of Analytical Chemistry (2010) from Xiamen University, China. He is currently an associate professor at China University of Petroleum (East China), and his research interests include the development of plasmonic nanomaterials for catalysis, plasmonic sensors for colorimetric detection of environmental pollutants, and the development of micro-extraction techniques for solvent-free sample pre-treatment.



Dr. Suresh C. Pillai obtained his PhD in the area of Nanotechnology from Trinity College Dublin and then performed a postdoctoral research at California Institute of Technology (Caltech), USA. Upon completion of this appointment he returned to Trinity College Dublin as a Research Fellow before joining CREST-DIT as a Senior Research Manager in April 2004. Suresh joined in IT Sligo as a Senior Lecturer in Environmental Nanotechnology in October 2013. He is an elected fellow of the UK's Royal Microscopical Society (FRMS) and the Institute of Materials, Minerals and Mining (FIMMM). Suresh was responsible for acquiring more than €3 million direct R&D funding. He is currently one of the editors of ESPR (Environmental Science and Pollution Research) and member of the Editorial Boards of a number of science and technology journals. He has published several scientific articles in leading peer reviewed journals and has presented in several international conferences. He has delivered over fifty international invited talks including several key-note and plenary talks. He was also the recipient of the 'Hothouse Commercialisation Award 2009' from the Minister of Science, Technology and Innovation and the recipient of the 'Enterprise Ireland Research Commercialization Award 2009'.

(Environmental Science and Pollution Research) and member of the Editorial Boards of a number of science and technology journals. He has published several scientific articles in leading peer reviewed journals and has presented in several international conferences. He has delivered over fifty international invited talks including several key-note and plenary talks. He was also the recipient of the 'Hothouse Commercialisation Award 2009' from the Minister of Science, Technology and Innovation and the recipient of the 'Enterprise Ireland Research Commercialization Award 2009'.



Dr. Yi Li obtained his Ph.D. degree from National University of Singapore in 2004. After that, he worked in Tsinghua University, China as a postdoc fellow. Dr. Li is currently a Professor of Environmental Engineering Program at the Hohai University, China. His research mainly focuses on sustainable water resource management and sustainable photocatalysis development. He teaches courses in the areas of wastewater treatment. Dr. Li is the author of > 100 referred journal publications and 36 patents. He is also the author of several book chapters. He was the recipient of National Natural Science Fund for Excellent Young Scholar, China (2013).



Shih-Hsin Ho is currently a Professor (Young Thousand Talents) of Environmental Science and Engineering at Harbin Institute of Technology, China, and a Chair Professor (Minjiang Scholar) at Fuzhou University, China. He is currently working on microalgae technology, biofuel production and wastewater treatment. He is currently served as the lead guest editor of Bioresources and Bioprocessing and advisory board members for several reputed journals. Dr. Ho has published > 90 refereed journal (SCI) publications, > 50 conference proceedings, > 3 professional book chapter publications, and > 20 presentations. His work received over 2200 citations with an H index of 26.



Dr. Dionysios (Dion) D. Dionysiou is currently a Professor of Environmental Engineering and Science Program at the University of Cincinnati. He teaches courses and performs research in the areas of drinking water quality and treatment, advanced oxidation technologies and nanotechnologies, and physical-chemical processes for water quality control. He is currently one of the editors of Chemical Engineering Journal, Editor-in-Chief of the Journal of Advanced Oxidation Technologies, Editor-in-Chief of the Journal of Environmental Engineering (ASCE), and member of the Editorial Boards of several other journals. Dr. Dionysiou is the author or co-author of > 360 refereed journal publications, > 86 conference proceedings, > 32 book chapter publications, > 26 editorials, and > 600 presentations. He has edited/co-edited 6 books on water quality, water reuse, ferrate/ferrite technologies, and photocatalysis. He is currently co-editing a book on harmful algal blooms. Dr. Dionysiou's work received over 20,000 citations with an H factor of 73.